

Safe Output Regulation of Coupled Hyperbolic PDE-ODE Systems [★]

Ji Wang ^a and Miroslav Krstic ^b

^a*Department of Automation, Xiamen University, Xiamen 361005, China*

^b*Department of Mechanical and Aerospace Engineering, University of California, San Diego, La Jolla, CA 92093-0411, USA*

Abstract

This paper presents a safe output regulation control strategy for a class of systems modeled by a coupled 2×2 hyperbolic PDE-ODE structure, subject to fully distributed disturbances throughout the system. A state-feedback controller is developed by the nonovershooting backstepping method to simultaneously achieve exponential output regulation and enforce safety constraints on the system output, which is the state furthest from the control input. To handle unmeasured PDE states and external disturbances, a state observer and a disturbance estimator are designed. Explicit bounds on the estimation errors are derived and used to construct a robust safe regulator that accounts for the uncertainties. The proposed control scheme guarantees that: 1) If the system output is initially within the safe region, it remains there; otherwise, it will be rescued to the safety within a prescribed time; 2) The output tracking error converges to zero exponentially; 3) The observer accurately estimates both the distributed states and external disturbances, with estimation errors converging to zero exponentially; 4) All signals in the closed-loop system remain bounded. The effectiveness of the proposed method is demonstrated through a UAV delivery scenario with a cable-suspended payload, where the payload is regulated to track a desired reference while avoiding collisions with barriers.

Key words: hyperbolic PDEs; safe control; output regulation; boundary control

1 Introduction

1.1 Output Regulation of Coupled Hyperbolic PDEs

The output regulation problem seeks to design the control law that ensures the system output tracks desired references and/or rejects undesired disturbances. In recent years, considerable attention has been devoted to output regulation for infinite-dimensional systems governed by partial differential equations (PDEs). Among various methodologies, the backstepping approach has emerged as a widely adopted and powerful framework, whose foundational development was established in [14]. Upon the backstepping-based boundary stabilization of 2×2 hyperbolic PDEs presented in [20] and [8], initial contributions toward backstepping-based output regulation for 2×2 hyperbolic PDEs appeared in [1]. Subsequent extensions to more general heterodirectional transport PDEs were proposed in [2], [11], and [27]. For wave-type PDEs, similar regulator designs were developed in [28] and [29]. Research efforts were also directed at PDE-ODE interconnected systems, which naturally arise in many applications. Backstepping boundary control designs for interconnected 2×2 hyperbolic PDEs and ODEs were proposed

in [17], and the ODE-PDE-ODE configurations were further addressed in [23], [21], [9], and [7]. Subsequently, the output regulation of hyperbolic PDEs sandwiched between two ODEs was explored in [31], and the regulation problems involving coupled wave PDE-ODE systems and hyperbolic PDEs coupled with nonlinear ODEs were investigated in [12] and [30], respectively.

Despite these advances, most existing works only focus on stabilization and output regulation goals without addressing safety constraints—that is, ensuring that the system output state remains within a predefined safe region during the regulating operation. In many applications, such as autonomous vehicles, robotics, and UAV systems, where collision avoidance is essential, safety is critical. Therefore, integrating output regulation objectives with safety guarantees for PDE systems, i.e., safe output regulation of PDEs, remains an open and significant research topic.

1.2 Safe Control

Control Barrier Functions (CBFs) have emerged as a powerful tool for safe control design, as introduced in [5], where system states are constrained to remain within a designated safe region by ensuring the non-negativity of an appropriately constructed CBF. To enforce this constraint within the closed-loop system, CBF-based control strategies are typi-

[★] The material in this paper was not presented at any conference.

Email addresses: jiwang@xmu.edu.cn (Ji Wang), krstic@ucsd.edu (Miroslav Krstic).

cally combined with a quadratic program (QP) safety filter, which overrides potentially unsafe nominal control inputs to generate safe control actions. High relative degree CBFs have been further developed in [18], [25], and [26], after the presence of non-overshooting control design techniques in [15]. Based on the tools developed in [15], mean-square stabilization of stochastic nonlinear systems toward an equilibrium on the barrier was achieved in [16], and prescribed-time safety (PTSF)—which guarantees safety over a user-specified finite time horizon—was proposed in [3].

However, safe control of PDE systems remains largely underexplored. The first result in this area was presented in [13], which proposed a CBF-based boundary control scheme for a Stefan model involving parabolic PDEs with actuator dynamics. The safe regulation of the hyperbolic PDEs was proposed in [24]. Yet, these approaches assume full-state availability and do not address output-feedback scenarios with external disturbances. Designing observer-based output-feedback safety controllers is challenging even for disturbed ODE systems, as ensuring safety in the presence of state estimation errors and external disturbances requires significant enhancements to the robustness of the CBF framework. These challenges become even more pronounced in PDE systems, making the development of output-feedback safe PDE control a highly nontrivial and largely open research problem.

1.3 Main Contributions

- 1) In contrast to traditional output regulation of hyperbolic PDEs [1], [11], [12], [31], our approach not only ensures that the system output tracks the desired trajectory but also guarantees that it stay within a prescribed safe region.
- 2) Compared to our previous work [24] on safe control of coupled hyperbolic PDEs, this paper presents several improvements: a) Beyond the state-feedback framework, a safe output-feedback controller is developed, which accounts for unmeasured PDE states and external disturbances during the safe regulation; b) Instead of restricting safety to positivity, a general barrier function h is introduced, enabling broader and more flexible safety specifications; c) If the system starts outside the safe set, the proposed controller guarantees that it will be rescued to the safety within a prescribed time that can be selected as a design parameter by the user.
- 3) To the best of our knowledge, this work presents the first result on safe output regulation for PDE systems. We apply the control input to a UAV that transports a cable-suspended payload, successfully regulating the payload at the bottom of the cable to track a desired reference while avoiding collisions with surrounding obstacles.

1.4 Notation

- The symbol \mathbb{N} denotes the set $\{1, 2, \dots\}$.
- We use the notation $L^2(0, 1)$ for the standard space of the equivalence class of square-integrable, measurable func-

tions $f : (0, 1) \rightarrow \mathbb{R}$, with $\|f\|^2 := \int_0^1 f(x)^2 dx < +\infty$ for $f \in L^2(0, 1)$.

- Let $u : \mathbb{R}_+ \times [0, 1] \rightarrow \mathbb{R}$ be given. We use the notation $u[t]$ to denote the profile of u at certain $t \geq 0$, i.e., $u[t] = u(x, t)$ for all $x \in [0, 1]$.
- Let $|Y|$ be Euclidean norm of the vector Y , and $\|A\|_2$ denotes the induced 2-norm of the matrix A .
- We define $\underline{x}_j := [x_1, x_2, \dots, x_j]^T$.

For ease of presentation, we omit or simplify the arguments of functions and functionals when no confusion arises. Besides, if $a > b$ happens in $\sum_{i=a}^b$ of this paper, it means that the result is zero.

2 Problem Formulation

2.1 Plant

The considered plant is

$$\dot{Y}(t) = AY(t) + Bw(0, t) + G_1d(t), \quad (1)$$

$$z_t(x, t) = -q_1z_x(x, t) + d_1w(x, t) + G_2(x)d(t), \quad (2)$$

$$w_t(x, t) = q_2w_x(x, t) + d_2z(x, t) + G_3(x)d(t), \quad (3)$$

$$z(0, t) = pw(0, t) + CY(t) + G_4d(t), \quad (4)$$

$$w(1, t) = qz(1, t) + G_5d(t) + U(t), \quad (5)$$

$\forall (x, t) \in [0, 1] \times [0, \infty)$, where the function $U(t)$ is the control input to be designed. The scalars $z(x, t) \in \mathbb{R}$, $w(x, t) \in \mathbb{R}$ are states of the PDEs, $Y^T(t) = [y_1, y_2, \dots, y_n] \in \mathbb{R}^n$ are ODE states. The disturbances $d(t) \in \mathbb{R}^{m_d \times 1}$ are unmeasurable. The plant parameters d_1, d_2 , the transport speed $q_1 > 0, q_2 > 0$, and the matrices $G_1 \in \mathbb{R}^{n \times m_d}, G_2, G_3 \in (C[0, 1])^{1 \times m_d}$ regarding the disturbance input locations, are known and arbitrary. The subsystem Y -ODE is strict-feedback linear, where the matrix A , the column vector B are in the form of

$$A = \begin{pmatrix} a_{1,1} & 1 & 0 & 0 & \cdots & 0 \\ a_{2,1} & a_{2,2} & 1 & 0 & \cdots & 0 \\ & & \vdots & & & \\ a_{n-1,1} & a_{n-1,2} & a_{n-1,3} & a_{n-1,4} & \cdots & 1 \\ a_{n,1} & a_{n,2} & a_{n,3} & a_{n,4} & \cdots & a_{n,n} \end{pmatrix}, \quad (6)$$

and $B = (0, 0, \dots, b)^T$, with arbitrary constants $a_{i,j}$, and $b > 0$ (without any loss of generality for $b < 0$). This indicates that the Y -ODE is in the controllable form which covers many practical models. The matrix $C \in \mathbb{R}^{1 \times n}$ is arbitrary satisfying that (A, C) is observable.

2.2 Exogenous signal model

Like many articles on output regulation [11], the reference and disturbance signals are considered to be generated by a

finite-dimensional exogenous model:

$$\dot{v}(t) = Sv(t), \quad t > t_0, \quad v(t_0) \in \mathbb{R}^{n_v} \quad (7)$$

where the spectrum $\sigma(S)$ of the known diagonalizable matrix $S \in \mathbb{R}^{n_r \times n_r}$ only contains eigenvalues on the imaginary axis, which allows the modelling of bounded and persistently acting exogenous signals. In particular, this signal model can generate the exogenous signals as constant or trigonometric functions of time as well as linear combinations of both signal forms. Defining $S = \text{bdiag}(S_r, S_d)$ with $S_r \in \mathbb{R}^{n_r \times n_r}$, $S_d \in \mathbb{R}^{n_d \times n_d}$, and $v = \text{col}(v_r, v_d)$ where $v_r \in \mathbb{R}^{n_r}$, $v_d \in \mathbb{R}^{n_d}$, one obtains the reference model and the disturbance model, respectively,

$$\dot{v}_r(t) = S_r v_r(t), \quad \dot{v}_d(t) = S_d v_d(t) \quad (8)$$

where $n_r + n_d = n_v$. Also, we have

$$d(t) = P_d v(t) = \bar{P}_d v_d(t), \quad P_d = \bar{P}_d E_d, \quad (9)$$

$$r(t) = P_r v(t) = \bar{P}_r v_r(t), \quad P_r = \bar{P}_r E_r, \quad (10)$$

where $P_d \in \mathbb{R}^{m_d \times n_v}$, $P_r \in \mathbb{R}^{1 \times n_v}$, $\bar{P}_d \in \mathbb{R}^{m_d \times n_d}$, $\bar{P}_r \in \mathbb{R}^{1 \times n_r}$, $E_r = [I_r, 0] \in \mathbb{R}^{n_r \times n_v}$, $E_d = [0, I_d] \in \mathbb{R}^{n_d \times n_v}$ where I_d, I_r are identity matrices with dimensions of n_d, n_r , respectively.

Assumption 1 $(S_d, (G_5 + G_4)\bar{P}_d)$ is controllable, (S_r, \bar{P}_r) is observable.

2.3 Control Objective

The output tracking error $e(t) = y_1(t) - r(t)$ of the system converges to zero while staying in the safe region in the sense that the time-varying barrier function $h(e(t), t)$ is non-negative, i.e., $h(e(t), t) \geq 0$. Because of the delay property of the transport PDE, there is no control for the distal ODE in the time interval $[t_0, \bar{t}_0]$, where t_0 is the initial time and \bar{t}_0 is the time when the control action begins to regulate the ODE, i.e.,

$$\bar{t}_0 = t_0 + \frac{1}{q_2} \quad (11)$$

namely, the initial regulation time. We impose the following assumption regarding the time-varying barrier function h for the output signal.

Assumption 2 The time-varying function h is n times differentiable with respect to each of its arguments, i.e., e as well as t , and satisfies that $\frac{\partial h(e, t)}{\partial e} \neq 0$, $\forall e \in \{\ell \in \mathbb{R} | h(\ell, t) \geq 0\}$, $t \in [\bar{t}_0, \infty)$ when h is positive at $t = \bar{t}_0$, or otherwise $\frac{\partial h(e, t)}{\partial e} \neq 0$, $\forall e \in \mathbb{R}$, $t \in [\bar{t}_0, \infty)$. Besides, $|h(e(t), t)| < \infty \Rightarrow |e(t)| < \infty$ and $\lim_{t \rightarrow \infty} h(e(t), t) = 0 \Rightarrow \lim_{t \rightarrow \infty} e(t) = 0$.

In Assumption 2, the fact $\lim_{t \rightarrow \infty} h(e(t), t) = 0 \Rightarrow \lim_{t \rightarrow \infty} e(t) = 0$ implies the prescribed safe region converges to the desired reference as $t \rightarrow \infty$, which is reasonable in the output regulation problem.

3 Nominal Safe Control Design

Applying (9), then (1)–(5) are rewritten as

$$\dot{Y}(t) = AY(t) + Bw(0, t) + \dot{G}_1 v(t), \quad (12)$$

$$z_t(x, t) = -q_1 z_x(x, t) + d_1 w(x, t) + \dot{G}_2(x) v(t), \quad (13)$$

$$w_t(x, t) = q_2 w_x(x, t) + d_2 z(x, t) + \dot{G}_3(x) v(t), \quad (14)$$

$$z(0, t) = pw(0, t) + CY(t) + \dot{G}_4 v(t), \quad (15)$$

$$w(1, t) = qz(1, t) + \dot{G}_5 v(t) + U(t), \quad (16)$$

where $\dot{G}_i = G_i P_d$, $i = 1, \dots, 5$. The matrixes $\dot{G}_i \in \mathbb{R}^{1 \times n_v}$, $i = 2, \dots, 5$ and $\dot{G}_1 := [\dot{g}_1; \dots; \dot{g}_n] \in \mathbb{R}^{n \times n_v}$ with $\dot{g}_j \in \mathbb{R}^{1 \times n_v}$, $j = 1, \dots, n$, are known.

3.1 First transformation

First, we propose the following transformation to derive and rewrite the tracking error dynamics in a form that will be helpful for the next transformation to barrier functions,

$$Z(t) = T_z Y(t) + T_v v(t), \quad (17)$$

where $Z(t) = [z_1, \dots, z_n]^T$ and the matrix $T_z \in \mathbb{R}^{n \times n}$ is

$$T_z = \begin{pmatrix} 1 & 0 & 0 & 0 & 0 \\ \varrho_{1,1} & 1 & 0 & 0 & 0 \\ \varrho_{2,1} & \varrho_{2,2} & 1 & 0 & 0 \\ \vdots & & & & \\ \varrho_{n-1,1} & \varrho_{n-1,2} & \dots & \varrho_{n-1,n-1} & 1 \end{pmatrix} \quad (18)$$

with the constants $\varrho_{i,j}$ defined by

$$\varrho_{1,1} = a_{1,1}, \quad (19)$$

$$\varrho_{2,1} = a_{2,1} + \varrho_{1,1} a_{1,1}, \quad \varrho_{2,2} = a_{2,2} + \varrho_{1,1} \quad (20)$$

and, for $i = 3, \dots, n$, by

$$\varrho_{i,1} = a_{i,1} + \sum_{j=1}^{i-1} \varrho_{i-1,j} a_{j,1}, \quad (21)$$

$$\varrho_{i,i} = a_{i,i} + \varrho_{i-1,i-1} + \sum_{j=i}^{i-1} \varrho_{i-1,j} a_{j,i}, \quad \forall i = 2, \dots, n-1, \quad (22)$$

$$\varrho_{i,i} = a_{i,i} + \varrho_{i-1,i-1}, \quad (23)$$

and where the matrix $T_v \in \mathbb{R}^{n \times n_v}$ is

$$T_v = -[P_r; \lambda_1 + P_r S^1; \dots; \lambda_{n-1} + P_r S^{n-1}] \quad (24)$$

with the vectors λ_i defined by

$$\lambda_0 = 0, \quad (25)$$

$$\lambda_i = - \sum_{j=1}^{i-1} \varrho_{i-1,j} \dot{g}_j - \dot{g}_i + \lambda_{i-1} S \quad \forall i = 1, \dots, n. \quad (26)$$

Applying the transformation (17), we now convert the Y -ODE (12) into

$$\dot{Z}(t) = A_Z Z(t) + B w(0, t) + B K^T Y(t) - \bar{G}_0 v(t) \quad (27)$$

where

$$A_Z = \begin{pmatrix} 0 & 1 & 0 & 0 & \cdots & 0 & 0 \\ 0 & 0 & 1 & 0 & \cdots & 0 & 0 \\ 0 & 0 & 0 & 1 & \cdots & 0 & 0 \\ \vdots & & & & & & \\ 0 & 0 & 0 & 0 & \cdots & 0 & 1 \\ 0 & 0 & 0 & \cdots & 0 & 0 & 0 \end{pmatrix} \quad (28)$$

and where

$$K^T = \frac{1}{b} [\varrho_{n,1}, \dots, \varrho_{n,n}]_{1 \times n}, \quad (29)$$

with $\bar{G}_0 = \frac{1}{b} B(\lambda_n + P_r S^n)$. Regarding Z -ODE in (27), z_1 is the tracking error that is to be regulated to zero, i.e.,

$$z_1(t) = e(t) \quad (30)$$

and the system matrix A_Z represents a chain-of-integrators which will be helpful for advancing to high-relative-order barrier functions in the next transformation. The details of the first transformation are shown in Appendix 0.1.

3.2 Second transformation

For the purpose of establishing barrier functions for the distal ODE, inspired by [3], we propose the following transformation

$$h_1(z_1(t), t) = h(e(t), t) + \sigma(t), \quad (31)$$

$$h_i(\underline{z}_i, t) = \sum_{j=1}^{i-1} \frac{\partial h_{i-1}}{\partial z_j} z_{j+1} + \frac{\partial h_{i-1}}{\partial t} + k_{i-1} h_{i-1}, \quad (32)$$

for $i = 2, 3, \dots, n$, with

$$\sigma(t) = \begin{cases} e^{\frac{1}{t_a^2}} (-h(e(\bar{t}_0), \bar{t}_0) + \epsilon) e^{\frac{-1}{(t - \bar{t}_0 - t_a)^2}}, & t \in [t_0, \bar{t}_0 + t_a], \\ 0, & t \geq \bar{t}_0 + t_a \\ \text{if } h(e(\bar{t}_0), \bar{t}_0) \leq 0, \\ 0, & t \geq t_0, \quad \text{if } h(e(\bar{t}_0), \bar{t}_0) > 0 \end{cases} \quad (33)$$

where t_a and ϵ are arbitrarily positive design parameters. The function $\sigma(t)$ is designed to address scenarios where the states are in the unsafe region at the initial regulation time \bar{t}_0 . Specifically, when the initial state $e(\bar{t}_0)$ fall outside the original safe region—indicated by the condition $(h(e(\bar{t}_0), \bar{t}_0) \leq 0)$ —a new barrier function is created to guide the state back to the original safe region. The constant ϵ indicates the distance from the safe barrier of the initial value of the new barrier function h_1 , and t_a is the upper bound of the time taken to rescue to the safe region. We only ensure the state, which falls into the unsafe region at the initial regulation time \bar{t}_0 , to rescue to safety within a prescribed time t_a , but not prescribed-time regulation to the safe boundary. The evolution of $e(t)$ on $t \in [t_0, \bar{t}_0]$ can be expressed as the initial states as

$$e(t_0 + a) = C_1 Z(t_0 + a) \quad (34)$$

$\forall a \in [0, \frac{1}{q_2}]$, where $Z(t_0 + a)$ is defined by (B.4) in Appendix 0.2, which is determined by the initial states $Y(t_0), w[t_0], z[t_0]$ and $v(t_0)$. Therefore, $h(e(\bar{t}_0), \bar{t}_0)$ can be determined by the initial states of the plant according to (34), denoted as

$$h(e(\bar{t}_0), \bar{t}_0) = \mathcal{P}(Y(t_0), z[t_0], w[t_0], v(t_0)) \quad (35)$$

where the function \mathcal{P} is determined by inserting (34) with $a = \frac{1}{q_2}$, i.e., $e(\bar{t}_0)$, into the barrier function $h(e, t)$. Note that $\sigma(t)$ is continuous and has continuous derivatives of all orders. Therefore, together with Assumption 2, $h_1(z_1(t), t)$ is n times differentiable with respect to each of its arguments, i.e., z_1 and t . Please also note that $\dot{h}(e(t), t)$ denotes full derivative with respect to t whose calculation using the chain rule, and $\frac{\partial h(e(t), t)}{\partial t}$ denotes partial derivative with respect to one of its variables t . Define

$$\frac{\partial h(e(t), t)}{\partial e(t)} := \vartheta(z_1(t), t), \quad (36)$$

because of $z_1(t) = e(t)$ (30). Considering the fact $\frac{\partial h_n}{\partial z_n} = \frac{\partial h_{n-1}}{\partial z_{n-1}} = \frac{\partial h_{n-2}}{\partial z_{n-2}} = \dots = \frac{\partial h_1}{\partial z_1} = \frac{\partial h}{\partial e} = \vartheta$ that is obtained from (32), using (32) for $i = n$, we have $\dot{h}_n(\underline{z}_n, t) + k_n h_n = b(\vartheta w(0, t) + f(\underline{y}_n(t), v(t), t) - \vartheta \frac{1}{b} (\lambda_n + P_r S^n) v(t) + \vartheta K^T Y(t))$, where

$$f(\underline{z}_n(t), t) = \frac{1}{b} \left(\sum_{j=1}^{n-1} \frac{\partial h_n}{\partial z_j} z_{j+1} + \frac{\partial h_n}{\partial t} + k_n \left[\sum_{j=1}^{n-1} \frac{\partial h_{n-1}}{\partial z_j} z_{j+1} + \frac{\partial h_{n-1}}{\partial t} + k_{n-1} h_{n-1} \right] \right). \quad (37)$$

Applying (31), (32) to convert (27) into

$$\dot{H}(t) = A_h H(t) + B \left(f(\underline{z}_n(t), t) + \vartheta w(0, t) \right)$$

$$-\vartheta \frac{1}{b} (\lambda_n + P_r S^n) v(t) + \vartheta K^T Y(t) \Big) \quad (38)$$

where

$$A_h = \begin{pmatrix} -k_1 & 1 & 0 & 0 & \cdots & 0 & 0 \\ 0 & -k_2 & 1 & 0 & \cdots & 0 & 0 \\ 0 & 0 & -k_3 & 1 & \cdots & 0 & 0 \\ & & & \vdots & & & \\ 0 & 0 & 0 & 0 & \cdots & 0 & 1 \\ 0 & 0 & 0 & 0 & \cdots & 0 & -k_n \end{pmatrix}. \quad (39)$$

This chain structure $\dot{H}(t) = A_h H(t)$, also known as the form of high relative-degree CBFs [18], [25], was proposed in [15] for the nonovershooting control.

3.3 Third transformation

In order to remove the in-domain coupling destabilizing terms from the 2×2 hyperbolic PDE system and cancel the extra terms in (27), we propose the following backstepping transformations:

$$\begin{aligned} \alpha(x, t) &= z(x, t) - \int_0^x \phi(x, y) z(y, t) dy \\ &\quad - \int_0^x \varphi(x, y) w(y, t) dy - \gamma(x) Y(t) - \bar{\gamma}(x) v(t) - q(x, t), \end{aligned} \quad (40)$$

$$\begin{aligned} \beta(x, t) &= w(x, t) - \int_0^x \Psi(x, y) z(y, t) dy \\ &\quad - \int_0^x \Phi(x, y) w(y, t) dy - \lambda(x) Y(t) - \bar{\lambda}(x) v(t) - p(x, t) \end{aligned} \quad (41)$$

where $\phi, \varphi, \gamma, \bar{\gamma}, \Psi, \Phi, \lambda, \bar{\lambda}$ are defined in Appendix 0.3, and where $p(x, t)$ and $q(x, t)$ satisfy

$$p_t(x, t) = q_2 p_x(x, t), \quad p(0, t) = \frac{-1}{\vartheta(z_1(t), t)} f(z_n, t), \quad (42)$$

$$q_t(x, t) = -q_1 q_x(x, t), \quad q(0, t) = p * p(0, t). \quad (43)$$

The solution p is

$$p(x, t) = \frac{-1}{\vartheta(z_1(t + \frac{x}{q_2}), t + \frac{x}{q_2})} f\left(z_n(t + \frac{x}{q_2}), t + \frac{x}{q_2}\right) \quad (44)$$

where $\vartheta(z_1(t + \frac{x}{q_2}), t + \frac{x}{q_2})$ is nonzero according to Assumption 2. The solution (44) is determined by the prediction $Z(t + \frac{x}{q_2})$ given by (B.4) that is expressed by the current states $Y(t), w[t], z[t]$ and $v(t)$ recalling (17) to replace $Z(t)$

with $Y(t)$. By (40), (41), the system (2)–(5) with (27) is converted into

$$\dot{H}(t) = A_h H(t) + B \vartheta(z_1(t), t) \beta(0, t), \quad (45)$$

$$\alpha(0, t) = p \beta(0, t), \quad (46)$$

$$\alpha_t(x, t) = -q_1 \alpha_x(x, t), \quad (47)$$

$$\beta_t(x, t) = q_2 \beta_x(x, t), \quad (48)$$

$$\beta(1, t) = 0 \quad (49)$$

by choosing the control input as

$$\begin{aligned} U(t) &= -qz(1, t) + \int_0^1 \Psi(1, y) z(y, t) dy \\ &\quad + \int_0^1 \Phi(1, y) w(y, t) dy + \lambda(1) Y(t) \\ &\quad - (\dot{G}_5 - \bar{\lambda}(1)) v(t) + p(1, t) \end{aligned} \quad (50)$$

where $p(1, t)$ is given by (31)–(33), (37), (44), (B.4), $\Psi(1, y), \Phi(1, y), \lambda(1)$ are determined by (C.16)–(C.21), and $\bar{\lambda}(1)$ is given by (C.12), (C.13), that is,

$$\begin{aligned} p(1, t) &= \frac{-f(\varphi_1(Z(t), z[t], w[t], v(t), \frac{1}{q_2}), t + \frac{1}{q_2})}{\vartheta(C_1 \varphi_1(Z(t), z[t], w[t], v(t), \frac{1}{q_2}), t + \frac{1}{q_2})} \\ &:= g(Z(t), z[t], w[t], v(t), t) \\ &= g(T_z Y(t) + T_v v(t), z[t], w[t], v(t), t). \end{aligned} \quad (51)$$

3.4 Selection of safe design parameters

The design parameters $k_i, i = 1, 2, \dots, n-1$ satisfy

$$k_i > \max\{0, \bar{k}_i\} \quad (52)$$

where

$$\bar{k}_i(v(t_0)) = \frac{-1}{h_i(\underline{z}_i(\bar{t}_0), \bar{t}_0)} \left(\sum_{j=1}^i \frac{\partial h_i}{\partial z_j} z_{j+1}(\bar{t}_0) + \frac{\partial h_i}{\partial t} \right), \quad (53)$$

where, by (B.4) and (17), $Z(\bar{t}_0)$ can be expressed as the initial states $z[t_0], w[t_0], Y(t_0)$ and $v(t_0)$. We write $\bar{k}_i(v(t_0))$ in (53) to emphasize that it depends on the unknown initial values $v(t_0)$ of the external signal, which will be dealt with in the next section. The gain condition (52), (53) for the nonovershooting control ensures the following lemma.

Lemma 1 *With the design parameters $\kappa_i, i = 1, \dots, n-1$ satisfying (52), the high-relative-degree ODE CBFs is initialized positively, i.e., $h_i(\underline{z}_i(\bar{t}_0), \bar{t}_0) > 0, i = 1, \dots, n$.*

Proof. According to (31) and (33), we know $h_1(z_1(\bar{t}_0), \bar{t}_0) > 0$. Recalling (32), we have $h_i(\underline{z}_i(\bar{t}_0), \bar{t}_0) = \sum_{j=1}^{i-1} \frac{\partial h_{i-1}}{\partial z_j} z_{j+1}(\bar{t}_0) + \frac{\partial h_{i-1}}{\partial t} + k_{i-1} h_{i-1}(\underline{z}_{i-1}(\bar{t}_0), \bar{t}_0), i = 2, 3, \dots, n$. The lemma is thus obtained recalling (52). \square

We give the following definition about the safe initial condition, which is the sufficient and necessary condition under which the output state stays in the safe region before the control input arrives at the distal ODE subsystem. It is the counterpart to the initial state restriction, i.e., Assumption 1, in the work [4] about safe control with delays.

Definition 1 The safe initial condition is defined as $\varphi(Y(t_0), z[t_0], w[t_0], v(t_0), a) \geq 0$ for $a \in [0, \frac{1}{q_2}]$ and $\varphi(Y(t_0), z[t_0], w[t_0], v(t_0), \frac{1}{q_2}) \neq 0$, where the function φ is given by (B.5).

This definition is the sufficient and necessary condition of $h(e(t), t) \geq 0$ for $t \in [t_0, \bar{t}_0]$, i.e., the safety holds for the uncontrolled period at the beginning, and $h(e(\bar{t}_0), \bar{t}_0) \neq 0$ which means that the state does not stay at the safe boundary at the initial regulation time $t = \bar{t}_0$ for the distal ODE.

3.5 Result of the state-feedback safe control

Theorem 1 For initial data $w[t_0] \in L^2(0, 1)$, $z[t_0] \in L^2(0, 1)$, $Y(t_0) \in \mathbb{R}^n$, for design parameters κ_i , $i = 1, \dots, n-1$ satisfying (52), the closed-loop system including the plant (1)–(5) with the controller (50) has the properties:

1) There exists a unique solution $w[t] \in L^2(0, 1)$, $z[t] \in L^2(0, 1)$, $Y(t) \in \mathbb{R}^n$ to the system (1)–(5) under the control input (50).

2) Tracking error $e(t) = y_1(t) - r(t)$ is convergent to zero and all states are bounded;

3) Safety is ensured in the sense that:

a) When the safe initial condition in Definition 1 is satisfied, the safety is ensured from $t = t_0$, i.e., $h(e(t), t) \geq 0$, $\forall t \geq t_0$;

b) When the safe initial condition in Definition 1 is not satisfied, and $h(e(\bar{t}_0), \bar{t}_0) > 0$, the safety is ensured from $t = \bar{t}_0$, i.e., $h(e(t), t) \geq 0$, $\forall t \geq \bar{t}_0$;

c) When the safe initial condition in Definition 1 is not satisfied, and $h(e(\bar{t}_0), \bar{t}_0) \leq 0$, the state will return and stay in the safe region no later than a finite time $\bar{t}_0 + t_a$ where a constant $t_a > 0$ can be arbitrarily assigned by users, i.e., $h(e(t), t) \geq 0$, $\forall t \geq \bar{t}_0 + t_a$.

Proof. 1) For the given initial conditions, recalling Assumption 2 and the transformations (17), (31)–(33), (40), (41), we have $\beta[t_0] \in L^2(0, 1)$, $\alpha[t_0] \in L^2(0, 1)$, $H(t_0) \in \mathbb{R}^n$. Considering the target system (45)–(49), it is followed that there exists a unique solution $\beta[t] \in L^2(0, 1)$, $\alpha[t] \in L^2(0, 1)$, $H(t) \in \mathbb{R}^n$. According to (32), we have $\frac{\partial h_i}{\partial z_{i-1}} = \frac{\partial h_{i-1}}{\partial z_{i-2}} + \frac{\partial h_{i-1}}{\partial z_{i-1} \partial t} + k_{i-1} \frac{\partial h_{i-1}}{\partial z_{i-2}} = \frac{\partial h_{i-1}}{\partial z_{i-1}} + k_{i-1} \frac{\partial h_1}{\partial z_1} + \frac{\partial h_1}{\partial z_1 \partial t} = \frac{\partial h_2}{\partial z_1} + \frac{\partial h_1}{\partial z_1} \sum_{j=2}^{j=i-1} k_j + (i-2) \frac{\partial h_1}{\partial z_1 \partial t} = \frac{\partial h_1}{\partial z_1} \sum_{j=1}^{j=i-1} k_j + (i-1) \frac{\partial h_1}{\partial z_1 \partial t}$, $\forall i \geq 2$. Recursively, we obtain $\sum_{i=1}^n \sum_{j=1}^i |\frac{\partial h_i}{\partial z_j}| \leq \mathcal{M}(|\frac{\partial h_1}{\partial z_1}| + \sum_{j=1}^{n-1} |\frac{\partial h_1}{\partial z_1 \partial t^{n-1}}|)$ for some positive constant \mathcal{M} . Recalling Assumption 2, (31), and (33) that renders that σ has continuous derivatives of all orders, we know $\frac{\partial h_i}{\partial z_j}$, $1 \leq j \leq i \leq n$, $i, j \in \mathbb{N}$ are bounded. According to (31), (33), and Assumption 2, recursively applying (32), we obtain from $H(t) \in \mathbb{R}^n$ that $Z(t) \in \mathbb{R}^n$. It is then obtained that $Y(t) \in \mathbb{R}^n$, recalling (17). According

to the theory of Volteral integral equations [32], considering the backstepping transformation (40), (41) as well as the boundedness and continuity of the kernels given in Appendix 0.3, there exists a bounded and continuous the kernel $\mathcal{K}(x, y)$ such that

$$\begin{aligned} \begin{pmatrix} z(x, t) \\ w(x, t) \end{pmatrix} &= \begin{pmatrix} \alpha(x, t) \\ \beta(x, t) \end{pmatrix} + \int_0^x \mathcal{K}(x, y) \begin{pmatrix} \alpha(y, t) \\ \beta(y, t) \end{pmatrix} dy \\ &+ \mathcal{K}_1(x)Y(t) + \mathcal{K}_2(x)v(t) + \begin{pmatrix} q(x, t) \\ p(x, t) \end{pmatrix} \\ &+ \int_0^x \mathcal{K}(x, y) \begin{pmatrix} q(y, t) \\ p(y, t) \end{pmatrix} dy \end{aligned} \quad (54)$$

where $\mathcal{K}(x, y)$ can be computed from the kernels $\phi, \varphi, \Psi, \Phi$, and where $\mathcal{K}_1(x) = (\gamma(x), \lambda(x))^T + \int_0^x \mathcal{K}(x, y) (\gamma(y), \lambda(y))^T dy$, $\mathcal{K}_2(x) = (\bar{\gamma}(x), \bar{\lambda}(x))^T + \int_0^x \mathcal{K}(x, y) (\bar{\gamma}(y), \bar{\lambda}(y))^T dy$. According to the exogenous signal defined in Sec. 2.2, we have $v(t) \in \mathbb{R}^{n_v}$. Applying (54), together with (42), (43), Property 1 is obtained.

2) Recalling the target system (45)–(49) and Assumption 2 indicates that ϑ is bounded, by the method of characteristics, it is obtained that $\beta[t], \alpha[t], H(t)$ are bounded all the time, and moreover, $\beta[t] \equiv 0$, $\alpha[t] \equiv 0$ for $t \geq \frac{1}{q_1} + \frac{1}{q_2}$ and $|H(t)|$ is exponentially convergent to zero recalling the fact that A_h defined in (39) is Hurwitz. We then obtain from (31), (33), and Assumption 2 that z_1 is bounded. Recursively applying (32), recalling the fact that $\frac{\partial h_i}{\partial z_j}$, $1 \leq j \leq i \leq n$, $i, j \in \mathbb{N}$ are bounded, which is obtained in the proof of property 1, we obtain $|Z(t)|$ is bounded. Recalling (17) and the boundedness of $|v(t)|$ straightforwardly obtained for Sec. 2.2, we have that $|Y(t)|$ is bounded. Applying the Cauchy-Schwarz inequality into the inverse transformation (54), we have that $z[t], w[t]$ are bounded. Besides, it is obtained from the exponential convergence to zero of h_1 that $h(e, t)$ is exponentially convergent to zero according to (31) and (33) that shows $\sigma(t) \equiv 0$ after a finite time $t = \bar{t}_0 + t_a$. Recalling Assumption 2, we know $e(t)$ is exponentially convergent to zero. Property 2 is obtained.

3) According to the choice of the design parameters κ_i , $i = 1, \dots, n-1$ in (52), recalling Lemma 1, we know $h_i > 0$ at $t = \bar{t}_0 = \frac{1}{q_2}$. Because $\beta(0, t) \equiv 0$ for $t \geq \frac{1}{q_2}$ considering the target system (45)–(49), and the system matrix A_h defined in (39) represents a form of high-relative-degree CBFs h_i as presented in [15], [18], we have $h_i > 0$ for $t \geq \bar{t}_0$. Based on this, we prove the safety in cases a)–c) as follows: a) When the initial safe condition in Definition 1 is satisfied, we know from the fact $h(e(\bar{t}_0), \bar{t}_0) > 0$ that $\sigma(t) \equiv 0$ according to (33). Therefore, it is obtained from $h_1 > 0$ for $t \geq \bar{t}_0$ and (31) that $h(e(t), t) > 0$ for $t \geq \bar{t}_0$. Thus, together with fact that $h(e(t), t) \geq 0$ holds on $t \in [t_0, \bar{t}_0]$; ensured by the initial safe condition in Definition 1, we have that $h(e(t), t) \geq 0$ holds on $t \in [\bar{t}_0, \infty)$.

b) When the safe initial conditions in Definition 1 is not satisfied, if $h(e(\bar{t}_0), \bar{t}_0) > 0$, through the same process with the proof in a), we have $h(e(t), t) \geq 0$ holds on $t \in [\bar{t}_0, \infty)$;
c) When the safe initial conditions in Definition 1 is not satisfied, if $h(e(\bar{t}_0), \bar{t}_0) \leq 0$, it is followed that $\sigma(t) \equiv 0$ after a finite time $t = \bar{t}_0 + t_a$ according to (33) where $t_a > 0$ is a free design parameter. We then obtain from the fact $h_1 > 0$ for $t \geq \bar{t}_0$ and (31) that $h(e(t), t) \geq 0$ for $t \geq \bar{t}_0 + t_a$. Property 3 is thus obtained. The proof of this theorem is complete. \square

4 Unmeasured Distributed States and Unknown External Disturbances

4.1 State observer and disturbance estimator

In the last section, we have proposed the nominal control design on the basis of a completely known model. In practice, the distributed states in PDE, and also the external disturbances, are always inaccessible. Therefore, we use the measurements at the boundaries, i.e., $Y(t)$, $z(1, t)$, together with the known reference signal $r(t)$, to build the state and disturbance observer to estimate the unmeasured distributed states and the unknown external disturbance:

$$\dot{\hat{v}}_r = S_r \hat{v}_r(t) + L_r(r(t) - \bar{P}_r \hat{v}_r(t)), \quad (55)$$

$$\dot{\hat{v}}_d = S_d \hat{v}_d(t) + L_d(z(1, t) - \hat{z}(1, t)), \quad (56)$$

$$\begin{aligned} \hat{z}_t(x, t) = & -q_1 \hat{z}_x(x, t) + d_1 \hat{w}(x, t) + \bar{G}_2(x) \hat{v}_d(t) \\ & + L_1(x)(z(1, t) - \hat{z}(1, t)), \end{aligned} \quad (57)$$

$$\begin{aligned} \hat{w}_t(x, t) = & q_2 \hat{w}_x(x, t) + d_2 \hat{z}(x, t) + \bar{G}_3(x) \hat{v}_d(t) \\ & + L_2(x)(z(1, t) - \hat{z}(1, t)), \end{aligned} \quad (58)$$

$$\hat{z}(0, t) = p w(0, t) + C Y(t) + \bar{G}_4 \hat{v}_d(t), \quad (59)$$

$$\hat{w}(1, t) = q z(1, t) + U(t) + \bar{G}_5 \hat{v}_d(t), \quad (60)$$

with the initial states $\hat{z}[t_0]$, $\hat{w}[t_0]$, $\hat{v}(t_0)$ chosen in the known bounds given in Assumptions 3, 4, where $[\hat{v}_r, \hat{v}_d]$ is the estimate of $v^T = [v_r, v_d]$, and \hat{z} , \hat{w} are observer states. $\bar{G}_i = G_i \bar{P}_d$, $i = 2, 3, 4, 5$. The vector L_r is selected such that $S_r - L_r \bar{P}_r$ Hurwitz, considering that (S_r, \bar{P}_r) is observable, and observer gains L_d , $L_1(x)$, $L_2(x)$ are defined later. Define the estimation error states

$$(\tilde{v}_r, \tilde{v}_d, \tilde{z}, \tilde{w}) = (v_r, v_d, z, w) - (\hat{v}_r, \hat{v}_d, \hat{z}, \hat{w}), \quad (61)$$

we obtain the observer error system:

$$\dot{\tilde{v}}_r = (S_r - L_r \bar{P}_r) \tilde{v}_r, \quad (62)$$

$$\dot{\tilde{v}}_d = S_d \tilde{v}_d(t) - L_d \tilde{z}(1, t), \quad (63)$$

$$\begin{aligned} \tilde{z}_t(x, t) = & -q_1 \tilde{z}_x(x, t) + d_1 \tilde{w}(x, t) \\ & + \bar{G}_2 \tilde{v}_d(t) - L_1(x) \tilde{z}(1, t), \end{aligned} \quad (64)$$

$$\begin{aligned} \tilde{w}_t(x, t) = & q_2 \tilde{w}_x(x, t) + d_2 \tilde{z}(x, t) \\ & - L_2(x) \tilde{z}(1, t) + \bar{G}_3 \tilde{v}_d(t), \end{aligned} \quad (65)$$

$$\tilde{z}(0, t) = p \tilde{w}(0, t) + \bar{G}_4 \tilde{v}_d(t), \quad (66)$$

$$\tilde{w}(1, t) = \bar{G}_5 \tilde{v}_d(t), \quad (67)$$

recalling (1)–(5), (8)–(10). Applying the transformation:

$$\begin{aligned} \tilde{z}(x, t) = & \tilde{\alpha}(x, t) - \int_x^1 K^{11}(x, y) \tilde{\alpha}(y, t) dy \\ & - \int_x^1 K^{12}(x, y) \tilde{\beta}(y, t) dy, \end{aligned} \quad (68)$$

$$\begin{aligned} \tilde{w}(x, t) = & \tilde{\beta}(x, t) - \int_x^1 K^{21}(x, y) \tilde{\alpha}(y, t) dy \\ & - \int_x^1 K^{22}(x, y) \tilde{\beta}(y, t) dy \end{aligned} \quad (69)$$

where $K^{11}(x, y)$, $K^{12}(x, y)$, $K^{21}(x, y)$, $K^{22}(x, y)$ on $\{(x, y) | 0 \leq x \leq y \leq 1\}$ satisfy $q_1 K_x^{11}(x, y) + q_1 K_y^{11}(x, y) = d_1 K^{21}(x, y)$, $q_1 K_x^{12}(x, y) - q_2 K_y^{12}(x, y) = d_1 K^{22}(x, y)$, $q_2 K_x^{21}(x, y) - q_1 K_y^{21}(x, y) = -d_2 K^{11}(x, y)$, $q_2 K_x^{22}(x, y) + q_2 K_y^{22}(x, y) = -d_2 K^{12}(x, y)$, $K^{21}(x, x) = \frac{-d_2}{q_1 + q_2}$, $K^{12}(x, x) = \frac{d_1}{q_1 + q_2}$, $K^{11}(0, y) = p K^{21}(0, y)$, $K^{22}(0, y) = \frac{1}{p} K^{12}(0, y)$, whose solution is in the same form as (C.18), (C.19) (which can be seen clearly by changing the domain from $\{(x, y) | 0 \leq x \leq y \leq 1\}$ to $\{(x, y) | 0 \leq y \leq x \leq 1\}$ and comparing it with (B.4)–(B.6) of [24]), and choosing the observer gains as

$$\begin{aligned} L_1(x) = & -p_1(x) + \int_x^1 K^{11}(x, y) p_1(y) dy \\ & + \int_x^1 K^{12}(x, y) p_2(y) dy - q_1 K^{11}(x, 1), \end{aligned} \quad (70)$$

$$\begin{aligned} L_2(x) = & -p_2(x) + \int_x^1 K^{21}(x, y) p_1(y) dy \\ & + \int_x^1 K^{22}(x, y) p_2(y) dy - q_1 K^{21}(x, 1), \end{aligned} \quad (71)$$

where $p_1(x)$, $p_2(x)$ are to be determined later, then (63)–(67) is converted into

$$\dot{\tilde{v}}_d = S_d \tilde{v}_d(t) - L_d \tilde{\alpha}(1, t), \quad (72)$$

$$\tilde{\alpha}_t(x, t) = -q_1 \tilde{\alpha}_x(x, t) + \bar{K}_2(x) \tilde{v}_d(t) + p_1(x) \tilde{\alpha}(1, t), \quad (73)$$

$$\tilde{\beta}_t(x, t) = q_2 \tilde{\beta}_x(x, t) + \bar{K}_1(x) \tilde{v}_d(t) + p_2(x) \tilde{\alpha}(1, t), \quad (74)$$

$$\tilde{\beta}(1, t) = \bar{G}_5 \tilde{v}_d(t), \quad (75)$$

$$\tilde{\alpha}(0, t) = p \tilde{\beta}(0, t) + \bar{G}_4 \tilde{v}_d(t), \quad (76)$$

where $\bar{K}_1(x)$, $\bar{K}_2(x)$ satisfy $\bar{K}_1(x) - \int_x^1 K^{22}(x, y) \bar{K}_1(y) dy - \int_x^1 K^{21}(x, y) \bar{K}_2(y) dy - q_2 K^{22}(x, 1) \bar{G}_5 - \bar{G}_3(x) = 0$, and $\bar{K}_2(x) - \int_x^1 K^{11}(x, y) \bar{K}_2(y) dy - \int_x^1 K^{12}(x, y) \bar{K}_1(y) dy - q_2 K^{12}(x, 1) \bar{G}_5 - \bar{G}_2(x) = 0$.

Applying the second transformation:

$$\bar{\alpha}(x, t) = \tilde{\alpha}(x, t) - \Lambda(x) \tilde{v}_d(t), \quad (77)$$

$$\bar{\beta}(x, t) = \tilde{\beta}(x, t) - \Lambda_1(x) \tilde{v}_d(t), \quad (78)$$

where $\Lambda_1(x)$, $\Lambda(x)$ satisfy $q_2\Lambda'_1(x) - \Lambda_1(x)S_d + \bar{K}_1(x) = 0$, $\Lambda_1(1) = \bar{G}_5$, $q_1\Lambda'(x) + \Lambda(x)S_d - \bar{K}_2(x) = 0$, $\Lambda(0) = p\Lambda_1(0) + \bar{G}_4$, and defining $p_1(x)$, $p_2(x)$ in the observer gains (70), (71) are $p_1(x) = -\Lambda(x)L_d$, $p_2(x) = -\Lambda_1(x)L_d$, then (72)–(76) is converted into

$$\dot{\tilde{v}}_d = (S_d - L_d\Lambda(1))\tilde{v}_d(t) - L_d\bar{\alpha}(1, t), \quad (79)$$

$$\bar{\alpha}_t(x, t) = -q_1\bar{\alpha}_x(x, t), \quad (80)$$

$$\bar{\beta}_t(x, t) = q_2\bar{\beta}_x(x, t), \quad (81)$$

$$\bar{\beta}(1, t) = 0, \quad (82)$$

$$\bar{\alpha}(0, t) = p\bar{\beta}(0, t), \quad (83)$$

where L_d is chosen such that $S_d - L_d\Lambda(1)$ Hurwitz. The final target observer error system we arrive at is (79)–(83) with (62). Before presenting the results, we propose the following lemma and assumptions that will be used in establishing the result about the observer error system.

Lemma 2 *For a Hurwitz matrix A_H , we have the following estimate*

$$\|e^{A_H t}\|_2 \leq M_H(t)e^{-\sigma_1 t}, \forall t \geq 0 \quad (84)$$

where $\sigma_1 = -\max \Re \lambda(A_H)$, and where $M_H = \|P_1\|_2 \|P_1^{-1}\|_2 > 0$ which is constant when A_H is diagonalizable, otherwise, $M_H(t) = \|P_1\|_2 \|P_1^{-1}\|_2 \sum_{j=0}^{n_k} \frac{t^j}{j!} > 0$ which is a polynomial in t . The matrix P_1 is invertible, satisfying

$$A_H = P_1 \Lambda P_1^{-1} \quad (85)$$

where Λ is either a diagonal matrix (if A_H is diagonalizable) or a Jordan matrix (in which the size of the largest Jordan block is n_k).

Proof. The proof is shown in the Appendix 0.4. \square

For the observer-based output-feedback control in this section, we require the following assumptions. Assumptions 3, 4 indicate the bounds of the initial values of the unmeasured PDE states and the disturbances are known, but arbitrary, which will be used in estimating the upper bounds of the observer errors required in building the output-feedback safe controller in the next subsection.

Assumption 3 *The bounds of initial states are known and arbitrary, i.e., $(z[t_0], w[t_0]) \in \mathcal{D}$, where $\mathcal{D} = \{(\ell_1(x), \ell_2(x)) | \underline{z}_0(x) \leq \ell_1(x) \leq \bar{z}_0(x), \underline{w}_0(x) \leq \ell_2(x) \leq \bar{w}_0(x)\}$. The functions $\underline{z}_0(x)$, $\bar{z}_0(x)$, $\underline{w}_0(x)$, $\bar{w}_0(x)$, are known and arbitrary.*

Assumption 4 *The initial values of disturbances satisfy $v(0) \in \mathcal{D}_v$, where $\mathcal{D}_v = \{(\ell_1, \dots, \ell_{n_v}) \in \mathbb{R}^{n_v} | v_i \leq \ell_i(0) \leq \bar{v}_i, i = 1, 2, \dots, n_v\}$, especially, $v_d(0) \in \mathcal{D}_d$ where $\mathcal{D}_d = \{(\ell_1, \dots, \ell_{n_d}) \in \mathbb{R}^{n_d} | v_i \leq \ell_i(0) \leq \bar{v}_i, i = 1, 2, \dots, n_d\}$.*

Assumption 5 *The sign of $h(e(\bar{t}_0), \bar{t}_0)$ is known.*

For Assumption 5, the exact value of $h(e(\bar{t}_0), \bar{t}_0)$ is not required but its sign that will be used in determining the form of σ in (33), which can be judged based on the known bounds of the initial values in Assumptions 3, 4.

Assumption 6 *The time-varying function h is n times differentiable with respect to each of its arguments, i.e., e as well as t , and satisfies that $\frac{\partial h(e, t)}{\partial e}$ is continuous as well as $\frac{\partial h(e, t)}{\partial e} \neq 0$, $\forall e \in \mathbb{R}$, $t \in [t_0, \infty)$. Besides, $|h(e(t), t)| < \infty \Rightarrow |e(t)| < \infty$ and $\lim_{t \rightarrow \infty} h(e(t), t) = 0 \Rightarrow \lim_{t \rightarrow \infty} e(t) = 0$. Also, the barrier function h ensures that there exists a positive ξ_e such that*

$$\begin{aligned} & |g(T_z Y(t) + T_v v(t), z[t], w[t], v(t), t) \\ & - g(T_z \tilde{Y}(t) + T_v \tilde{v}(t), \tilde{z}[t], \tilde{w}[t], \tilde{v}(t), t)| \\ & \leq \xi_e (|\tilde{v}(t)| + \|\tilde{z}\| + \|\tilde{w}\|) \end{aligned} \quad (86)$$

where g are determined by h via (51), (37), (31), (32), and (36).

Due to the uncertainties of the plant state and the external disturbances, this assumption about the barrier function h is less general than Assumption 2. This assumption can be verified easily when planning the barrier function h using (37) (31), (32).

Defining the observer error norm

$$\tilde{\Omega}_e = \|\tilde{z}(\cdot, t)\| + \|\tilde{w}(\cdot, t)\| + |\tilde{v}|, \quad (87)$$

whose upper bound is estimated in the following lemma, which will be used in building the output-feedback safe controller.

Lemma 3 *For initial data $\tilde{w}[0] \in L^2(0, 1)$, $\tilde{z}[0] \in L^2(0, 1)$, $\tilde{Y}(0) \in \mathbb{R}^n$, $\tilde{v}_d(0) \in \mathbb{R}^{n_d}$, $\tilde{v}_r(0) \in \mathbb{R}^{n_r}$, with the observer (55)–(60) where the observer gains $L_1(x)$, $L_2(x)$ are defined by (70), (71), and L_d , L_r satisfies that $S_d - L_d\Lambda(1)$ as well as $S_r - L_r\bar{P}_r$ are Hurwitz, respectively, the observer error system (62)–(67) is well-posed in the sense of $\tilde{w}[t] \in L^2(0, 1)$, $\tilde{z}[t] \in L^2(0, 1)$, $\tilde{Y}(t) \in \mathbb{R}^n$, $\tilde{v}(t) \in \mathbb{R}^{n_v}$ for $t \in [t_0, \infty)$. Moreover, the exponential convergence to zero of the observer errors is achieved in the sense that*

$$\begin{aligned} \tilde{\Omega}_e & \leq \Upsilon_1 \bar{M}_d + (1 + \Upsilon_1) M_d + (1 + \Upsilon_1) M_0 M_r(t) e^{-\sigma_r t} \\ & := \rho_{e1}(t), \quad t \in [0, \frac{1}{q_1} + \frac{1}{q_2}), \end{aligned} \quad (88)$$

$$\begin{aligned} \tilde{\Omega}_e & \leq (1 + \Upsilon_1) (\bar{M}_d M_2(t) e^{-\sigma_e t} + M_0 M_r(t) e^{-\sigma_r t}) \\ & := \rho_{e2}(t), \quad t \in [\frac{1}{q_1} + \frac{1}{q_2}, \infty) \end{aligned} \quad (89)$$

where the positive constants \bar{M}_d , M_d , M_0 , \bar{M}_d , Υ_1 are defined by (E.22), (E.18), (E.16), (E.20), and (E.21), respectively, and where $M_r(t)$, σ_r as well as $M_e(t)$, σ_e are given by Lemma 2 with applying $A_H = S_d - L_d\Lambda(1)$ and $A_H = S_r - L_r\bar{P}_r$, respectively.

Proof. The proof is given in the Appendix 0.5. \square

4.2 Output-feedback safe control

Considering the uncertainties, the design parameters are chosen as

$$k_i > \max_{\ell \in \mathcal{D}_v} \{0, \bar{k}_i(\ell)\}, i = 1, 2, \dots, n-1 \quad (90)$$

where \bar{k}_i are defined in (52), and where \mathcal{D}_v denotes the bounds of the disturbances given in Assumption 4. Besides, there also exist conservatism in the choice of $\sigma(t)$, which arises from using known bounds to estimate the lower bound of $h(e(\bar{t}_0), \bar{t}_0)$, denoted as $\underline{h}(e(\bar{t}_0), \bar{t}_0) = \min_{\ell_1, \ell_2 \in \mathcal{D}, \ell_3 \in \mathcal{D}_v} \mathcal{P}(Y(t_0), \ell_1[t_0], \ell_2[t_0], \ell_3(t_0))$, where the function \mathcal{P} is defined in (35). The lower bound $\underline{h}(e(\bar{t}_0), \bar{t}_0)$ is used in place of $h(e(\bar{t}_0), \bar{t}_0)$ in the coefficient of the function $\sigma(t)$ (33) (the sign of $h(e(\bar{t}_0), \bar{t}_0)$ used in judging the case in (33) is known according to Assumption 5). Design the output-feedback safe controller as

$$U_f = \hat{U} + \text{sign}(\vartheta(t_0))\rho_e(t) \quad (91)$$

where \hat{U} is obtained by replacing the unmeasurable distributed states $z(x, t)$, $w(x, t)$, and the external disturbances $v(t)$ in the nominal control law (50) with their estimates,

and where the sign is defined by $\text{sign}(u) = \begin{cases} 1 & u \geq 0 \\ -1 & u < 0 \end{cases}$ and $\rho_e(t)$ is given by

$$\rho_e(t) = \begin{cases} 2 \max\{\|\Psi(1, y)\|, \|\Phi(1, y)\|, |\dot{G}_5 + \lambda(1)|, \xi_e\} \rho_{e1}, \\ 0 \leq t < \frac{1}{q_1} + \frac{1}{q_2}; \\ 2 \max\{\|\Psi(1, y)\|, \|\Phi(1, y)\|, |\dot{G}_5 + \lambda(1)|, \xi_e\} \rho_{e2}, \\ t \geq \frac{1}{q_1} + \frac{1}{q_2}. \end{cases} \quad (92)$$

The constant ξ_e is defined in Assumption 6. The functions ρ_{e1} and ρ_{e2} , which are the upper bounds of observer errors, are given by (88), (89) in Lemma 3. As will be seen clearly later, the function $\rho_e(t)$ is indeed an estimated upper bound of the error between the state-feedback and output-feedback controllers. The role of $\text{sign}(\vartheta(t_0))\rho_e(t)$ in (91) is to tolerate the estimation errors that arise from the unmeasured distributed states and the external disturbances by shrinking the original safe set to a subset that converges to the original safe set as time approaches infinity.

Remark 1 Even though there is a switch in (92), this discontinuity can be avoided in the practical implementation by picking a function $\rho_c = M_c e^{-\sigma_c t}$ satisfying $\rho_c \geq \rho_e$, at the cost of increasing the conservative, i.e., shrinking the safe region.

Theorem 2 For initial data $w[t_0] \in L^2(0, 1)$, $z[t_0] \in L^2(0, 1)$, $Y(t_0) \in \mathbb{R}^n$, $v(t_0) \in \mathbb{R}^{n_v}$, $\hat{w}[t_0] \in L^2(0, 1)$, $\hat{z}[t_0] \in L^2(0, 1)$, $\hat{v}(t_0) \in \mathbb{R}^{n_v}$ for design parameters κ_i , $i = 1, \dots, n-1$ satisfying (90), the closed-loop system including the plant (1)–(5), the observer (55)–(60), and the controller U_f (91) ensures:

1) There exists a unique solution $w[t] \in L^2(0, 1)$,

$z[t] \in L^2(0, 1)$, $\hat{w}[t] \in L^2(0, 1)$, $\hat{z}[t] \in L^2(0, 1)$, $Y(t) \in \mathbb{R}^n$, $v(t) \in \mathbb{R}^{n_v}$, $\hat{v}(t) \in \mathbb{R}^{n_v}$, to the output-feedback closed-loop system;

2) Tracking error $e(t) = y_1(t) - r(t)$ is convergent to zero and all states are bounded;

3) Safety is ensured in the sense that:

- a) When the safe initial condition in Definition 1 is satisfied, the safety is ensured from $t = t_0$, i.e., $h(e(t), t) \geq 0$, $\forall t \geq t_0$;
- b) When the safe initial condition in Definition 1 is not satisfied, and $h(e(\bar{t}_0), \bar{t}_0) > 0$, the safety is ensured from $t = \bar{t}_0$, i.e., $h(e(t), t) \geq 0$, $\forall t \geq \bar{t}_0$;
- c) When the safe initial condition in Definition 1 is not satisfied, and $h(e(\bar{t}_0), \bar{t}_0) \leq 0$, the state will return and stay in the safe region no latter than a finite time $\bar{t}_0 + t_a$ where the constant $t_a > 0$ can be arbitrarily assigned by users, i.e., $h(e(t), t) \geq 0$, $\forall t \geq \bar{t}_0 + t_a$.

Proof. 1) Define difference between U and \hat{U} is

$$\begin{aligned} \eta_e(t) &= U - \hat{U} \\ &= - \int_0^1 \Psi(1, y) \tilde{z}(y, t) dy - \int_0^1 \Phi(1, y) \tilde{w}(y, t) dy \\ &\quad - (\dot{G}_5 + \bar{\lambda}(1)) \tilde{v}(t) - \tilde{p}(1, t). \end{aligned} \quad (93)$$

Applying the controller (91), we have

$$\beta(1, t) = \text{sign}(\vartheta(z_1(t_0), t_0))\rho_e(t) - \eta_e(t). \quad (94)$$

The target system becomes (45)–(48) with (94). Considering the given initial condition and the transformations (40), (41) together with (44), (37), as well as the exogenous signal model (7), we have $\beta[t_0] \in L^2(0, 1)$, $\alpha[t_0] \in L^2(0, 1)$ and $v(t) \in \mathbb{R}^{n_v}$. We know from Lemma 3, (51), (86) in Assumption 6, and (92), (93) that $\text{sign}(\vartheta(z_1(t_0), t_0))\rho_e(t) - \eta_e(t)$ is bounded, and then we have $\beta[t] \in L^2(0, 1)$, $\alpha[t] \in L^2(0, 1)$, $H(t) \in \mathbb{R}^n$. Applying the transformation (54), through the same process in the proof of property 1 in Theorem 1, we have $w[t] \in L^2(0, 1)$, $z[t] \in L^2(0, 1)$, $Y(t) \in \mathbb{R}^n$. Recalling the results about the observer errors in Lemma 3, and the definition (61), Property 1 is obtained.

2) Recalling (93), (51), and (86) in Assumption 6, applying Lemma 3, we obtain

$$|\eta_e(t)| \leq 2 \max\{\|\Psi(1, y)\|, \|\Phi(1, y)\|, |\dot{G}_5 + \lambda(1)|, \xi_e\} \tilde{\Omega}_e(t) \leq \rho_e(t) \quad (95)$$

where $\tilde{\Omega}_e(t)$ is defined in (87). We know from (92) and Lemma 3 that $\rho_e(t)$ is exponentially convergent to zero, and thus $\text{sign}(\vartheta(z_1(t_0), t_0))\rho_e(t) - \eta_e(t)$ in (94) is exponentially convergent to zero as well recalling (95). Through the same process in the proof of the property 2 in Theorem 1, Property 2 is obtained.

3) The sign of ϑ is the same as its initial value at t_0 because of the fact that ϑ is continuous and not zero in Assumption 6 (recalling (36)). It is obtained from (94), (95) and (48), (45)

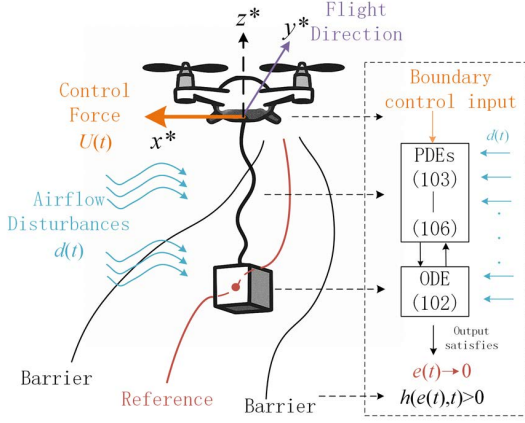


Fig. 1. UAV delivery with cable-suspended payloads.

that $\vartheta\beta(0, t) \geq 0$ for $t \in [\bar{t}_0, \infty)$. The choice of the design parameters k_i in (90) is a subset of the ones (52), which thus ensures $h_i > 0$ at $t = \bar{t}_0$ according to Lemma 1. Considering the system matrix A_h defined in (39) being a high-relative-degree CBFs h_i , we have $h_i > 0$ for $t \geq \bar{t}_0$. Then, through the same proof as the ones of cases a)–c) of the property 3 in Theorem 1, Property 3 is obtained. \square

5 Application in UAV Safe Delivery

In the simulation, we apply our control design to a UAV system with cable-suspended payloads for delivery as shown in Fig. 1, aiming to regulate the payload at the lower end of the cable to track a desired reference while avoiding collisions of the payload with surrounding barriers. For simplicity, we consider only one-dimensional motion.

5.1 Model

We adopt the following simplification in modeling: a) We neglect the UAV dynamics, assuming that the control force is applied directly at the top of the cable. However, if the UAV dynamics are taken into account, an additional ODE will be incorporated into the input channel. The corresponding controller can then be designed by combining the results from [24] for "sandwich" PDE systems. b) Assuming the UAV is flying at a predetermined speed along the y^* direction, we only focus on the safe regulation problem in the x^* direction. Then, according to [21], the oscillatory dynamics of the cables are modeled by wave PDEs, while the lumped payload at the cable tip is described by a linear ODE. Additionally, wind disturbances f_i , which act throughout the cable-payload system, are also taken into account. Thus, the mathematical model is formulated as follows:

$$M_0 \ddot{y}_1(t) = -d_0 \dot{y}_1(t) + T_0 u_x(0, t) + f_1(t), \quad (96)$$

$$u(0, t) = b_0(t), \quad (97)$$

$$\rho u_{tt}(x, t) = T_0 u_{xx}(x, t) - d_c u_t(x, t) + f_2(x, t), \quad (98)$$

$$T_0 u_x(L, t) = U(t) + f_3(t), \quad (99)$$

Table 1
Physical parameters

| Parameters (units) | values |
|--|--------|
| Cable length L (m) | 1 |
| Cable linear density ρ (kg/m) | 0.5 |
| Payload mass M_L (kg) | 15 |
| Gravitational acceleration g (m/s ²) | 9.8 |
| Cable material damping coefficient d_c (N·s/m) | -1 |
| Damping coefficient at payload d_0 (N·s/m) | -1 |

Note: anti-damping is introduced to increase challenges.

for $x \in [0, L]$. Therein, the function $u(x, t)$ represents the distributed transverse displacement along the cable, while $y_1(t)$ is the transverse displacement of the payload. The constant $T_0 = M_L g$ denotes the static tension. The terms f_i denote airflow disturbances, which will be given in detail later. The values of the physical parameters are listed in Tab. 1. To evaluate the controller under more demanding conditions, we intentionally introduce anti-damping, making the simulation model open-loop unstable. In this setting, instability sources are present in both PDE and ODE subsystems. Applying Riemann transformations

$$z(x, t) = u_t(x, t) - \sqrt{\frac{T_0}{\rho}} u_x(x, t), \quad (100)$$

$$w(x, t) = u_t(x, t) + \sqrt{\frac{T_0}{\rho}} u_x(x, t) \quad (101)$$

and defining a new variable $Y(t) = [y_1(t), \dot{y}_1(t)]^T$, (96)–(99) can be rewritten as

$$\dot{Y}(t) = AY(t) + Bw(0, t) + G_1 d(t), \quad (102)$$

$$z(0, t) = pw(0, t) + CX(t) + G_4 d(t), \quad (103)$$

$$z_t(x, t) = -q_1 z_x(x, t) + cz(x, t) + cw(x, t) + G_2(x) d(t), \quad (104)$$

$$w_t(x, t) = q_2 w_x(x, t) + cz(x, t) + cw(x, t) + G_3(x) d(t), \quad (105)$$

$$w(L, t) = qz(L, t) + G_5 d(t) + U(t), \quad (106)$$

where $q_1 = q_2 = \sqrt{\frac{T_0}{\rho}}$, $c = \frac{-d_c}{2\rho}$, $p = q = 1$, $A = [0, 1; 0, \frac{-d_0}{M_0} - \frac{\sqrt{T_0\rho}}{M_0}]$, $B = [0, \frac{\sqrt{T_0\rho}}{M_0}]^T$, $C = [0, 2]$. After the transformation (100), (101), the airflow disturbances f_i in the wave PDEs is given by the external disturbances $d(t) = \bar{P}_d v_d(t)$ (9) with $\bar{P}_d = I_{4 \times 4}$ and

$$v_d = [\sin(0.25t), \cos(0.25t), \sin(0.5t), \cos(0.5t)] \quad (107)$$

in the 2×2 hyperbolic PDEs (102)–(106), where $G_1 = [g_1, g_2]^T$, $g_1 = [1, 0, 0, 0]$, $g_2 = [1, 1, 1, 1]$, $G_4 = [0, 1, 0, 1]$, $G_5 = [1, 0, 1, 0]$, $G_2(x) = [x, 0, 0, 0]$, $G_3(x) = [0, x, 0, 0]$. The desired reference is set as $r(t) = \sin(0.25\pi t) +$

$\cos(0.25\pi t)$, i.e., $\bar{P}_r = [1, 1]$, and

$$v_r = [\sin(0.25\pi t), \cos(0.25\pi t)] \quad (108)$$

in (10). Therefore, the system matrix of exogenous signal model is $S_d = [0, 0.25, 0, 0; -0.25, 0, 0, 0; 0, 0, 0, 0.5; 0, 0, -0.5, 0]$ and $S_r = [0, 0.25\pi; -0.25\pi, 0]$.

Remark 2 Compared to the plant described by (1)–(5), the simulation model represented by (102)–(106) includes additional terms, specifically $c_1 z(x, t)$ and $c_2 w(x, t)$ in (104) and (105), respectively. However, these additions do not alter the state-feedback control design presented in this paper. To be exact, applying state-feedback control, the target system defined by (45) and (49), which corresponds to the closed-loop system, remains unchanged except for the updates that (47) and (48) are modified to $\beta_t = q_2 \beta_x + c\beta$ and $\alpha_t = -q_1 \alpha_x + c\alpha$. These modifications clearly do not impact the safety and stability results obtained. The only change in the observer-based output-feedback controller is adding the terms $c\hat{z}(x, t)$ and $c_2\hat{w}(x, t)$ in (57) and (58) of the observer, while all other aspects remain unchanged.

The initial values are defined as $w(x, 0) = \cos(2\pi x)$, $z(x, 0) = \sin(3\pi x)$, $y_2(0) = 0$, $\hat{w}(x, 0) = \cos(2\pi x) + 0.5$, $\hat{z}(x, 0) = \sin(3\pi x) + 0.5$, $\hat{v}_d(0) = [0.5, 1.5, 0.5, 1.5]^T$, $\hat{v}_r(0) = [0.5, 1.5]^T$ where the initial estimation errors are 0.5. Especially, the values $y_1(t_0)$ will be given in the next subsections. The simulation is conducted using the finite difference method with the space step as 0.05 and the time space 0.001.

5.2 Controller and simulation results

We test our safe controller in the following two cases. In Case 1, the safe region is on one side of the desired reference of the UAV, i.e., the reference is indeed the barrier; In Case 2, the barriers exist on both sides of the UAV's desired reference.

5.2.1 Case 1. One side of the desired reference is obstructed.

The barrier function is set as $h(e(t), t) = e(t) = y_1(t) - r(t)$, where $r(t)$ is the desired reference of UAV, and where the region above $r(t)$ is safe. Then we know $\vartheta = \frac{\partial h(e(t), t)}{\partial e} = 1$. According to (31)–(33), we have $h_1 = z_1(t) + \sigma(t)$, $h_2 = z_2(t) + \sigma(t) + k_1 z_1(t) + k_1 \sigma(t)$, where $\sigma(t)$ is given by (33) with choosing $\epsilon = 2$ and $t_a = 2$. According to (37), $f(z_n(t), t)$ is obtained as, $f(z_n(t), t) = \frac{1}{b}((k_1 + k_2)z_2 + k_1 k_2 z_1 + \ddot{\sigma}(t) + (k_1 + k_2)\dot{\sigma}(t) + k_1 k_2 \sigma(t))$. Then $p(1, t)$ can be obtained by recalling (51) that uses (B.4). Then the state-feedback controller is obtained recalling (50), where the design parameters are chosen as $k_1 = 1.5$, $k_2 = 4$, and the output-feedback controller U_f is obtained applying (91) with choosing the control design parameters $k_1 = 3$, $k_2 = 4$, $M_c = 15$, $\sigma_c = 2$ recalling Remark 1, and the observer design parameters $L_d = [10, 8, 10, 8]$, $L_r = [2, 1]$. For safe initialization, we set $y_1(t_0) = 8$. For the unsafe initialization

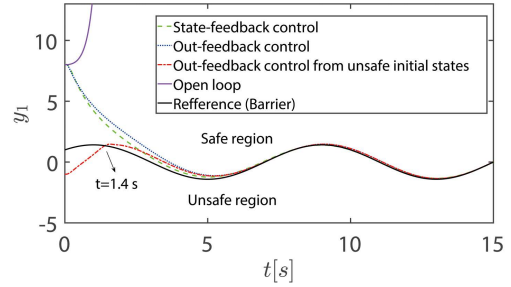


Fig. 2. Payload displacement y_1

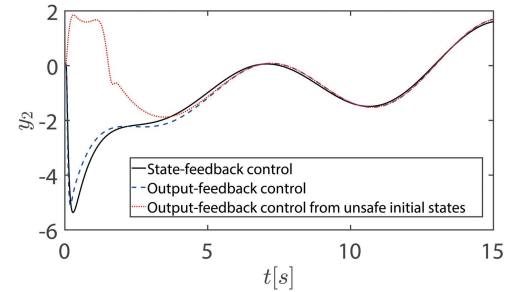


Fig. 3. Payload velocity y_2

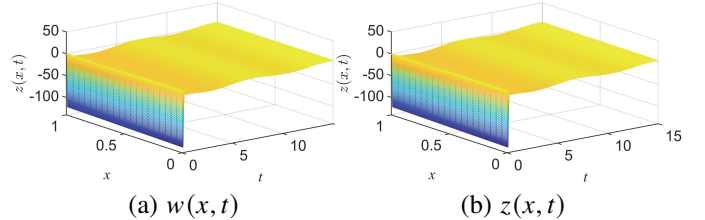


Fig. 4. PDE states with the output-feedback control.

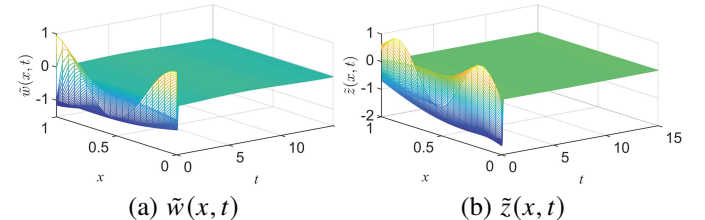


Fig. 5. Observer errors

case, we set $y_1(t_0) = -1$ that is beyond the safe region, and the design parameters in the output-feedback control law are the same as the output-feedback control in the safe initialization except for k_1, k_2 that are chosen as $k_1 = 2.5$, $k_2 = 4.5$ now, and additionally choosing $t_a = 2$, $\epsilon = 2$ in (33) to enforce the out return to the safe region. The simulation results are presented below. We know from the open-loop responses of y_1 in Fig. 2 that the plant is open-loop unstable, while both state-feedback control and output-feedback control achieve effective safe regulation—tracking the reference and ensuring the position of the payload stays within the safe region. Moreover, when y_1 starts outside the

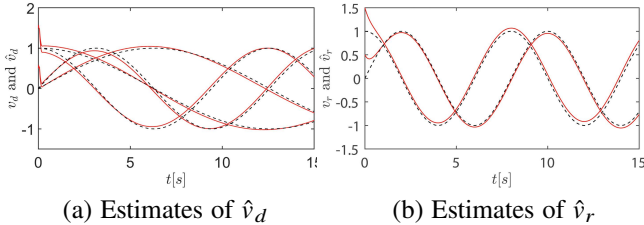


Fig. 6. Estimates of exogenous signals v_d , v_r in (107), (108) (red lines are estimates and dashed black lines are true values).

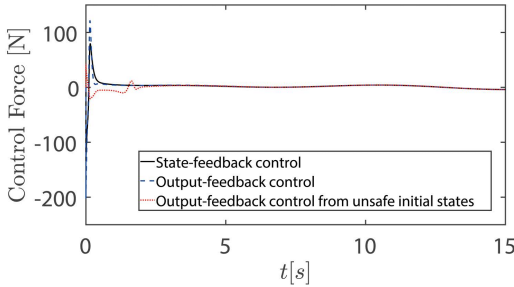


Fig. 7. Control forces at the top of the cable

safe region, the designed control input effectively guides it back to safety within 1.4 seconds, which is less than the designated time $\bar{t}_0 + t_a = 2.058$ in the control design. Another ODE state y_2 , i.e., the payload velocity, is shown in Fig. 3, and the PDE states that reflect the oscillations along the cable are given in Fig. 4 (where we only show the case that the output-feedback control from safe initial states for avoiding repetition), demonstrating the boundedness of these signals. We know from Figs 5, 6 that the observer can successfully track the unmeasured PDE states and the exogenous signals v_d and v_r . The control inputs in the above three situations are given in Fig. 7.

5.2.2 Case 2. Barriers are on both sides of the desired reference.

The barrier function is set as

$$h(e(t), t) = \delta(t) - |e(t)| = \delta(t) - |y_1(t) - r(t)| \quad (109)$$

where the time-varying function $\delta(t)$ is $\delta(t) = 15e^{-0.5t}$. It means that the reference trajectory of UAV payload is $r(t)$ and the safe region is within the two barriers: $r(t) + \delta(t)$ and $r(t) - \delta(t)$.

Remark 3 Because h is not differentiable at $e = 0$, the condition in Assumption 6 is not strictly satisfied by (109). However, the controller remains valid by explicitly defining $\frac{\partial h(e, t)}{\partial e} = -1$ when $e = 0$, i.e., $\vartheta(e(t), t) = -1$ for $e(t) > 0$ and $\vartheta(e(t), t) = 1$ for $e(t) \leq 0$. The signal ϑ is now discontinuous at $e = 0$, violating the continuity requirement in Assumption 6. This implies that $\text{sign}(\vartheta(z_1(t_0), t_0))$ in the output-feedback controller is not guaranteed to be invariant as in the proof of Theorem 2. Nevertheless, with appropriate observer gains L_d , L_r chosen via pole placement, the

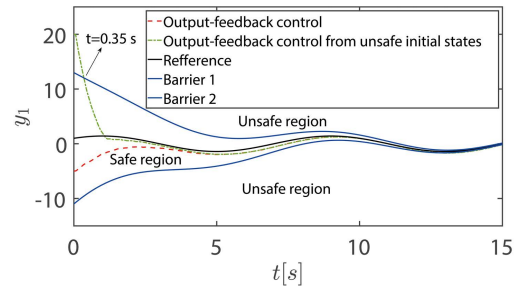


Fig. 8. Payload displacement y_1

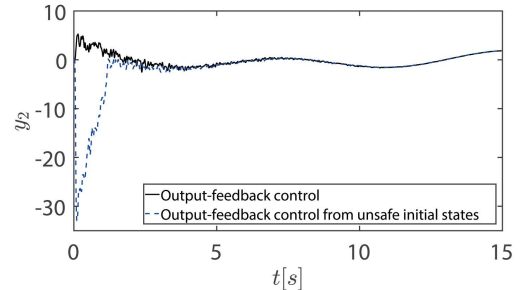


Fig. 9. Payload velocity y_2

observer errors can rapidly converge to zero, as shown in Fig., which means that $\rho_e(t)$ decays quickly to zero and the influence of the term $\text{sign}(\vartheta(z_1(t_0), t_0))\rho_e$ in the output-feedback controller becomes negligible after a short initial period. Therefore, the proposed control design remains valid without modification, as shown in the upcoming simulation results.

According to (31)–(33), we have $h_1 = -|z_1(t)| + \delta(t) + \sigma(t)$, $h_2 = \vartheta z_2 + \dot{\delta}(t) + \dot{\sigma}(t) - k_1|z_1(t)| + k_1\delta(t) + k_1\sigma(t)$, with $\sigma(t)$ is given by (33) with choosing $\epsilon = 2$ and $t_a = 2$. Recalling (37), we obtain f as $f(z_n(t), t) = \frac{1}{b}((k_1 + k_2)\vartheta z_2 - k_1 k_2|z_1(t)| + \ddot{\delta}(t) + (k_1 + k_2)\dot{\delta}(t) + k_1 k_2 \delta(t) + \dot{\sigma}(t) + (k_1 + k_2)\dot{\sigma}(t) + k_1 k_2 \sigma(t))$. Then $p(1, t)$ can be obtained by recalling (51) that uses (B.4). The output-feedback controller U_f is obtained applying (91), and recalling (50), with choosing the control design parameters $k_1 = 30$, $k_2 = 16$, $M_c = 20$, $\sigma_c = 1$ recalling Remark 1 and the observer design parameters $L_d = [10, 8, 10, 8]^T$, $L_r = [2, 1]^T$. For safe initialization, we set $y_1(t_0) = -5$. For unsafe initialization, we set $y_1(t_0) = 20$, which falls outside the safe region, where the design parameters remain the same as those used for the safe initialization. Additionally, we choose $t_a = 2$ and $\epsilon = 2$ in (33) to ensure that the system's output returns to the safe region. The simulation results are presented below. It is observed from Fig 8 that when y_1 , i.e., the position of the payload, starts within the safe region, it successfully tracks the reference meanwhile avoiding collisions with the barriers all the time; when the y_1 starts outside the safe region, it will return to the safe region at 0.35 s, which is less than $\bar{t}_0 + t_a = 2.058$, and also eventually follow the reference. The curves of y_2 and the PDE states are shown in Figs. 9,

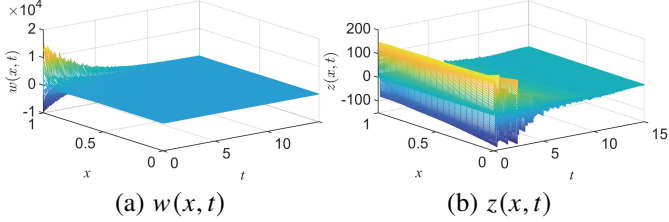


Fig. 10. PDE states with the output-feedback control.

10, which shows that these signals, i.e., the payload velocity and cable oscillations, are bounded, even though anti-damping is added to challenge the task. The results about the observer errors and the estimation errors of the external signals are similar to Figs. 5 and 6, which are not present here for avoiding repetition.

6 Conclusion

This paper has presented a safe output regulation strategy for a class of systems governed by coupled 2×2 hyperbolic PDE-ODE dynamics subject to fully distributed disturbances. By integrating the backstepping method with control barrier function (CBF) techniques, we developed a state-feedback controller that simultaneously enforces safety constraints and ensures exponential convergence of the system output to a desired reference. To address the challenges of unmeasured PDE states and external disturbances, a state observer and disturbance estimator were designed, with explicit bounds on estimation errors incorporated into the control law to ensure robust safety regulation under uncertainty. The resulting output-feedback controller guarantees that the system output remains within a general barrier-defined safe region if the initial condition is safe; otherwise, it is driven back into the safe region within a prescribed time set by the user. All closed-loop signals remain bounded, and the tracking error converges to zero exponentially. The effectiveness of the proposed framework is demonstrated through a UAV delivery scenario with a cable-suspended payload, highlighting its ability to achieve both precise trajectory tracking and reliable collision avoidance under wind disturbances. In future work, safe output regulation control of a class of parabolic PDE-ODE systems will be studied.

Appendix

0.1 The calculation details in the first transformation

Step. 1 Considering the first equation in the equation set (17) with (18), (24), applying (10), we directly have $z_1(t) = y_1(t) - r(t) = e_1(t)$, i.e., (30).

Step. 2 Taking the time derivative of the first equation in the equation set (17) with (18), (24), applying Y -ODE (12) and v -ODE (7), recalling the second equation in the equation set (17) with (19), (25), (26) for $i = 1$, one thus obtains $\dot{z}_1(t) = \dot{y}_1(t) - P_r S v(t) = a_{11} y_1(t) + y_2 + \dot{g}_1 v(t) - P_r S v(t) = \varrho_{1,1} y_1 + y_2 - (\lambda_1 + P_r S) v(t) = z_2(t)$.

Step. 3 Taking the time derivative of the second equation in the equation set (17) with (18), (24), applying Y -ODE (12) and v -ODE (7), recalling the third equation in the equation set (17) with (20) and (25), (26) for $i = 2$, one obtains $\dot{z}_2(t) = \dot{y}_2(t) + \rho_{11} \dot{y}_1(t) - (P_r S + \lambda_1) S v(t) = a_{2,1} y_1 + a_{2,2} y_2 + y_3 + \dot{g}_2 v(t) + \rho_{11} a_{11} y_1(t) + \rho_{11} y_2 + \rho_{11} \dot{g}_1 v(t) - (P_r S + \lambda_1) S v(t) = \varrho_{2,1} y_1 + \varrho_{2,2} y_2 + y_3 - (\lambda_2 + P_r S^2) v(t) = z_3(t)$.

Step. 4 Similarly, taking the time derivative of the third equation in the equation set (17) with (18), (24), applying Y -ODE (12) and v -ODE (7), recalling the fourth equation in the equation set (17) with (21)–(23), (25), (26) for $i = 3$, one obtains $\dot{z}_3(t) = \dot{y}_3(t) + \sum_{j=1}^2 \varrho_{2,j} \dot{y}_j - (P_r S^2 + \lambda_2) S v(t) = y_4 + (a_{3,1} + \sum_{j=1}^2 \varrho_{2,j} a_{j,1}) y_1 + (a_{3,2} + \varrho_{2,1} + \varrho_{2,2} a_{2,2}) y_2 + (a_{3,3} + \varrho_{2,2}) y_3 + (\dot{g}_3 + \sum_{j=1}^2 \varrho_{2,j} \dot{g}_j - \lambda_2 S) v(t) - P_r S^3 v(t) = y_4 + \varrho_{3,1} y_1 + \varrho_{3,2} y_2 + \varrho_{3,3} y_3 - (\lambda_3 + P_r S^3) v(t) = z_4(t)$.

Step. 5 We make an induction hypothesis: for the transformation (17) with (18), (24), we have $\dot{z}_i(t) = z_{i+1}(t)$ for $i \geq 3$, under the coefficients $\varrho_{i,i}$, $i = 1, \dots, i$ and λ_i defined by (21)–(23), (26), respectively. We then prove that the induction step holds. Taking the time derivative of the $i+1$ th equation in the equation set (17) with (18), (24), applying Y -ODE (12) and v -ODE (7), we have

$$\begin{aligned}
\dot{z}_{i+1}(t) &= \dot{y}_{i+1} + \sum_{j=1}^i \varrho_{i,j} \dot{y}_j - (\lambda_i + P_r S^{(i)}) S v(t) \\
&= y_{i+2} + \sum_{j=1}^{i+1} a_{i+1,j} y_j + \sum_{j=2}^{i+1} \varrho_{i,j-1} y_j + \sum_{j=1}^i \sum_{j=1}^j \varrho_{i,j} a_{j,j} y_j \\
&\quad + [\dot{g}_{i+1} + \sum_{j=1}^i \varrho_{i,j} \dot{g}_j - \lambda_i S] v(t) - P_r S^{(i)} S v(t) \\
&= y_{i+2} + [a_{i+1,1} + \sum_{j=1}^i \varrho_{i,j} a_{j,1}] y_1 \\
&\quad + \sum_{i=2}^i [a_{i+1,i} + \varrho_{i,i-1} + \sum_{j=1}^i \varrho_{i,j} a_{j,i}] y_i + (a_{i+1,i+1} + \varrho_{i,i}) y_{i+1} \\
&\quad + [\dot{g}_{i+1} + \sum_{j=1}^i \varrho_{i,j} \dot{g}_j - \lambda_i S - P_r S^{(i+1)}] v(t). \tag{A.1}
\end{aligned}$$

Recalling $z_{i+2}(t)$ that is defined by the $i+2$ th equation in the equation set (17), for $\dot{z}_{i+1}(t) = z_{i+2}(t)$ to hold, we obtain that the $\varrho_{i+1,i}$, $i = 1, \dots, i+1$ and λ_{i+1} satisfy (21)–(23), (26) for $i+1$. Therefore, the induction step holds. Recalling the Steps 1–4, it follows that $\dot{z}_i(t) = z_{i+1}(t)$ hold for $i = 1, \dots, n-1$ via the transformation (17) with (18)–(26).

Step. 6 Taking the time derivative of the n th equation in the equation set (17) with (18), (24), one obtains $\dot{z}_n(t) = \dot{y}_n + \sum_{j=1}^{n-1} \varrho_{n-1,j} \dot{y}_j - (\lambda_{n-1} + P_r S^{(n-1)}) S v(t) = \sum_{j=1}^n a_{n,j} y_j(t) + \dot{g}_n v(t) + b w(0, t) + \sum_{j=1}^{n-1} \varrho_{n-1,j} (y_{j+1} + \sum_{j=1}^j a_{j,j} y_j + \dot{g}_j v(t)) - (\lambda_{n-1} + P_r S^{(n-1)}) S v(t)$. We thus arrive at $\dot{z}_n(t) = b w(0, t) + K^T Y(t) - [\lambda_n + P_r S^n] v(t)$ with $K^T = [\varrho_{n,1}, \dots, \varrho_{n,n}]_{1 \times n}$, recalling (21)–(23), (26) for n , which is the n th equation in the equation set (27) considering (28), (29), and the definition

of B and \bar{G}_0 .

0.2 The calculation of the prediction $Z(t + \frac{x}{q_2}), Y(t + \frac{x}{q_2})$

For (1)–(4), applying (17), and

$$\begin{aligned}\eta(x, t) &= w(x, t) - \int_0^x \Psi(x, y)z(y, t)dy \\ &\quad - \int_0^x \Phi(x, y)w(y, t)dy - \lambda(x)Y(t) - \bar{\lambda}(x)v(t)\end{aligned}\quad (\text{B.1})$$

where the kernels $\Psi, \Phi, \lambda, \bar{\lambda}$ are the same as ones that will be given in Appendix 0.3, i.e., (C.16), (C.17) with (C.18)–(C.21), and (C.10), (C.12), (C.13), we then have

$$\dot{Z}(t) = A_z Z(t) + B\eta(0, t), \quad (\text{B.2})$$

$$\eta_t(x, t) = q_2 \eta_x(x, t). \quad (\text{B.3})$$

We omit the right boundary condition of η because it is not required in the analysis here. Therefore, we have $Z(t + a) = e^{A_z a} Z(t) + \int_0^a e^{A_z(a-\tau)} B\eta(q_2\tau, t) d\tau$, for $0 \leq a \leq \frac{1}{q_2}$, i.e.,

$$\begin{aligned}Z(t + a) &= e^{A_z a} Z(t) + \frac{1}{q_2} \int_0^{aq_2} e^{A_z(a-\frac{\ell}{q_2})} B \left(w(\ell, t) \right. \\ &\quad \left. - \int_0^\ell \Psi(\ell, y)z(y, t)dy - \int_0^\ell \Phi(\ell, y)w(y, t)dy \right. \\ &\quad \left. - \lambda(\ell)Y(t) - \bar{\lambda}(\ell)v(t) \right) d\ell \\ &:= \varphi_1(Z(t), z[t], w[t], v(t), a),\end{aligned}\quad (\text{B.4})$$

for $0 \leq a \leq \frac{1}{q_2}$. Recalling (7), (17), we have

$$\begin{aligned}Y(t + a) &= T_z^{-1} Z(t + a) - T_z^{-1} T_v v(t + a) \\ &= T_z^{-1} \varphi_1(T_z Y(t) + T_v v(t), w[t], z[t], a) \\ &\quad - T_z^{-1} T_v e^{S a} v(t) \\ &:= \varphi(Y(t), z[t], w[t], v(t), a), \quad 0 \leq a \leq \frac{1}{q_2},\end{aligned}\quad (\text{B.5})$$

recalling (B.3), (B.1). Therefore, $Y(t + \frac{x}{q_2}), x \in [0, 1]$ can be determined by $Y(t), z[t], w[t], v(t)$ as (B.5) with replacing a by $\frac{x}{q_2}$.

0.3 Functions $\varphi, \phi, \Psi, \Phi, \gamma, \lambda, \bar{\gamma}, \bar{\lambda}$ in (40), (41)

By mapping (27), (2)–(4) and (45)–(48) with using (1), the conditions of the kernels $\varphi, \phi, \Psi, \Phi, \gamma$ and λ in the backstepping transformation (40), (41) are obtained as the following equations

$$q_2 \varphi_y(x, y) - q_1 \varphi_x(x, y) - d_1 \phi(x, y) = 0, \quad (\text{C.1})$$

$$q_1 \phi_x(x, y) + q_1 \phi_y(x, y) + d_2 \varphi(x, y) = 0, \quad (\text{C.2})$$

$$q_2 \Psi_x(x, y) - q_1 \Psi_y(x, y) - d_2 \Phi(x, y) = 0, \quad (\text{C.3})$$

$$q_2 \Phi_x(x, y) + q_2 \Phi_y(x, y) - d_1 \Psi(x, y) = 0, \quad (\text{C.4})$$

evolving in the triangular domain $\{(x, y) : 0 \leq y \leq x \leq 1\}$ with the boundary conditions

$$\varphi(x, x) = \frac{d_1}{q_1 + q_2}, \quad \Psi(x, x) = \frac{-d_2}{q_1 + q_2}, \quad (\text{C.5})$$

$$q_2 \varphi(x, 0) - q_1 p \phi(x, 0) = \gamma(x)B, \quad (\text{C.6})$$

$$q_2 \Phi(x, 0) - q_1 p \Psi(x, 0) = \lambda(x)B, \quad (\text{C.7})$$

where $\gamma(x), \lambda(x)$ satisfy

$$q_1 \gamma'(x) + \gamma(x)A + q_1 C \phi(x, 0) = 0, \quad (\text{C.8})$$

$$q_2 \lambda'(x) - \lambda(x)A - q_1 C \Psi(x, 0) = 0, \quad (\text{C.9})$$

$$\lambda(0) = -K^T, \quad (\text{C.10})$$

$$\gamma(0) = -p K^T + C, \quad (\text{C.11})$$

with K^T defined in (29). The equation set (C.1)–(C.7) is a well-known system of heterodirectional linear coupled hyperbolic PDEs-ODE system, whose well-posedness has been proved in [17]. The functions $\bar{\lambda}$ and $\bar{\gamma}$ satisfy the following two ODEs

$$\bar{\lambda}(0) = \frac{1}{b}(\lambda_n + P_r S^n), \quad (\text{C.12})$$

$$\begin{aligned}q_2 \bar{\lambda}'(x) - \bar{\lambda}(x)S - \lambda(x) \dot{G}_1 + \dot{G}_3(x) - \int_0^x \Phi(x, y) \dot{G}_3(y) dy \\ - \int_0^x \Psi(x, y) \dot{G}_2(y) dy - q_1 \Psi(x, 0) \dot{G}_4 = 0,\end{aligned}\quad (\text{C.13})$$

$$\bar{\gamma}(0) = \frac{p}{b}(\lambda_n + P_r S^n) - \dot{G}_4, \quad (\text{C.14})$$

$$\begin{aligned}-q_1 \bar{\gamma}'(x) - \bar{\gamma}(x)S - \gamma(x) \dot{G}_1 + \dot{G}_2(x) - \int_0^x \phi(x, y) \dot{G}_2(y) dy \\ - \int_0^x \varphi(x, y) \dot{G}_3(y) dy - q_1 \phi(x, 0) \dot{G}_4 = 0.\end{aligned}\quad (\text{C.15})$$

The control law requires the solution of $\Psi(x, y), \Phi(x, y)$, whose explicit solution is obtained as follows according to [24] where [19] has been used:

$$\Psi(x, y) = F(x, y) + \int_y^x L(x, r) F(r, y) dr, \quad (\text{C.16})$$

$$\Phi(x, y) = H(x, y) - L(x, y) + \int_y^x L(x, r) H(r, y) dr, \quad (\text{C.17})$$

where

$$\begin{aligned}F(x, y) &= \frac{-1}{p(q_1 + q_2)} \left[\frac{d_1 q_2}{p q_1} I_0 \left(\frac{2\sqrt{d_1 d_2}}{q_1 + q_2} \sqrt{(x-y)(\frac{q_1}{q_2}x+y)} \right) \right. \\ &\quad \left. + \sqrt{d_1 d_2} \frac{x-y}{\frac{q_1}{q_2}x+y} I_1 \left(\frac{2\sqrt{d_1 d_2}}{q_1 + q_2} \sqrt{(x-y)(\frac{q_1}{q_2}x+y)} \right) \right. \\ &\quad \left. + (p d_2 - \frac{d_1 q_2}{p q_1}) \Pi \left(\frac{p q_1 d_2}{q_2} \frac{x-y}{q_1 + q_2}, \frac{d_1}{p q_1} \frac{q_1 x + q_2 y}{q_1 + q_2} \right) \right],\end{aligned}\quad (\text{C.18})$$

$$\begin{aligned}
H(x, y) = & \frac{-1}{q_1 + q_2} \left[\frac{d_1}{p} I_0 \left(\frac{2\sqrt{d_1 d_2}}{q_1 + q_2} \sqrt{(x-y)(\frac{q_1}{q_2}x + y)} \right) \right. \\
& + \sqrt{d_1 d_2} \frac{\frac{q_1}{q_2}x + y}{x-y} I_1 \left(\frac{2\sqrt{d_1 d_2}}{q_1 + q_2} \sqrt{(x-y)(\frac{q_1}{q_2}x + y)} \right) \\
& \left. + \left(\frac{p d_2 q_1}{q_2} - \frac{d_1}{p} \right) \Pi \left(\frac{p q_1 d_2}{q_2} \frac{x-y}{q_1 + q_2}, \frac{d_1}{p q_1} \frac{q_1 x + q_2 y}{q_1 + q_2} \right) \right] \quad (\text{C.19})
\end{aligned}$$

with $I_j (j \geq 0)$ denoting the modified Bessel function of the first kind (of order j), and $\Pi(s_1, s_2) = e^{s_1+s_2} (1 - s_2 e^{-s_1} \int_0^1 e^{-\tau s_2} I_0(2\sqrt{\tau s_1 s_2}) d\tau)$, and where

$$L(x, y) = \frac{-1}{q_2} \lambda(x-y) B \quad (\text{C.20})$$

with λ given by the ODE

$$\begin{aligned}
& q_2 \lambda'(x) - \lambda(x) A - q_1 C \int_0^x \frac{-1}{q_2} \lambda(z) B F(x-z, 0) dz \\
& - q_1 C F(x, 0) = 0. \quad (\text{C.21})
\end{aligned}$$

0.4 The proof of Lemma 2

There always exists an invertible matrix P_1 such that (85) holds, where Λ is either a diagonal matrix (if A_H is diagonalizable) or a Jordan matrix. If Λ is a diagonal matrix, it is straightforward to obtain

$$\|e^{A_H t}\|_2 \leq \|P_1\|_2 \|P_1^{-1}\|_2 e^{-\sigma_1 t}, \forall t \geq 0. \quad (\text{D.1})$$

If Λ is a Jordan matrix, for a Jordan block J_k of size k in Λ and has a corresponding eigenvalue λ , we know $J_k = \lambda I_k + N_k$, where I_k is an identity matrix of size k , and where N_k is a matrix of all zeros except ones on the first super diagonal, which is a nilpotent matrix that vanishes after the k -th power. Because I_k, N_k commute, we have $e^{J_k t} = e^{\lambda I_k t} e^{N_k t} = e^{\lambda I_k t} \sum_{j=0}^k \frac{N_k^j t^j}{j!}$. Therefore, $\|e^{J_k t}\|_2 \leq \sum_{j=0}^k \frac{t^j}{j!} e^{-\lambda t}$, where $\|N_k^j\|_2 \leq 1$ for $j = 0, \dots, k$, is used. Considering the Jordan matrix, we thus have, $\|e^{\Lambda t}\|_2 \leq \sum_{j=0}^{n_k} \frac{t^j}{j!} e^{-\sigma_1 t}$, where n_k is the size of the largest Jordan block. Considering (85), we obtain

$$\|e^{A_H t}\|_2 \leq \|P_1\|_2 \|P_1^{-1}\|_2 \sum_{j=0}^{n_k} \frac{t^j}{j!} e^{-\sigma_1 t}, \quad \forall t \geq 0. \quad (\text{D.2})$$

Considering (D.1), (D.2), the lemma is obtained.

0.5 Proof of Lemma 3

1) For $t \in [0, \frac{1}{q_2}]$, the solution of (80)–(83) is

$$\bar{\beta}(x, t) = \bar{\beta}(x + tq_2, 0) \quad x < tq_2 \quad (\text{E.1})$$

$$\bar{\beta}(x, t) = 0 \quad x \geq tq_2 \quad (\text{E.2})$$

$$\bar{\alpha}(x, t) = \bar{\alpha}(x - tq_1, 0) \quad x > tq_1 \quad (\text{E.3})$$

$$\bar{\alpha}(x, t) = p \bar{\beta}\left(\frac{t - \frac{x}{q_1}}{q_2}, 0\right) \quad x \leq tq_1. \quad (\text{E.4})$$

Considering the initial condition, we know $\bar{\beta}[0] \in L^2(0, 1)$, $\bar{\alpha}[0] \in L^2(0, 1)$ recalling the inverse of (77), (78), (68), (69). It implies that $\bar{\beta}[t] \in L^2(0, 1)$, $\bar{\alpha}[t] \in L^2(0, 1)$ on $t \in [0, \frac{1}{q_2}]$. For $t \in (\frac{1}{q_2}, \frac{1}{q_2} + \frac{1}{q_1}]$, the solution of (80)–(83) is

$$\bar{\beta}(x, t) = 0 \quad (\text{E.5})$$

$$\bar{\alpha}(x, t) = \bar{\alpha}(x - (t - \frac{1}{q_2})q_1, \frac{1}{q_2}), \quad x > (t - \frac{1}{q_2})q_1 \quad (\text{E.6})$$

$$\bar{\alpha}(x, t) = 0, \quad x \leq (t - \frac{1}{q_2})q_1. \quad (\text{E.7})$$

Recalling $\bar{\beta}[\frac{1}{q_2}] \in L^2(0, 1)$, $\bar{\alpha}[\frac{1}{q_2}] \in L^2(0, 1)$ obtained above, we know $\bar{\beta}[t] \in L^2(0, 1)$, $\bar{\alpha}[t] \in L^2(0, 1)$ on $t \in [\frac{1}{q_2}, \frac{1}{q_2} + \frac{1}{q_1}]$. According to (62), (79), it is straightforward to know $\tilde{v}_d \in \mathbb{R}^{n_d}$, $\tilde{v}_r \in \mathbb{R}^{n_r}$. For $t \in [\frac{1}{q_1} + \frac{1}{q_2}, \infty)$, the observer error system (79)–(83) becomes

$$\dot{\tilde{v}}_d = (S_d - L_d \Lambda(1)) \tilde{v}_d(t), \quad (\text{E.8})$$

$$\dot{\tilde{Y}}(t) = (A - LC) \tilde{Y}(t) + M_1 \tilde{v}_d(t), \quad (\text{E.9})$$

$$\bar{\alpha}(x, t) = 0, \quad (\text{E.10})$$

$$\bar{\beta}(x, t) = 0. \quad (\text{E.11})$$

It is obvious that $\bar{\beta}[t] \in L^2(0, 1)$, $\bar{\alpha}[t] \in L^2(0, 1)$, $\tilde{Y}(t) \in \mathbb{R}^n$, $\tilde{v}_d(t) \in \mathbb{R}^{n_d}$ hold for $t \in [\frac{1}{q_1} + \frac{1}{q_2}, \infty)$. Therefore, we obtain the well-posedness stated in this lemma.

2) Next, we prove the estimate (61) holds, i.e., the upper bound of the estimation error. According to the theory of Volteral integral equations [32], considering (68), (69) and the continuous and bounded kernels $K^{11}, K^{12}, K^{21}, K^{22}$,

there exists $\mathcal{P}_1(x, y)$ such that $\begin{pmatrix} \tilde{\alpha}(x, t) \\ \tilde{\beta}(x, t) \end{pmatrix} = \begin{pmatrix} \tilde{z}(x, t) \\ \tilde{w}(x, t) \end{pmatrix} + \int_x^1 \mathcal{P}_1(x, y) \begin{pmatrix} \tilde{z}(y, t) \\ \tilde{w}(y, t) \end{pmatrix} dy := \mathcal{T}(\tilde{z}(\cdot, t), \tilde{w}(\cdot, t))$, where the continuous and bounded kernel $\mathcal{P}_1(x, y)$ can be computed from the kernels $K^{11}, K^{12}, K^{21}, K^{22}$. Therefore, we have

$$\begin{aligned}
\begin{pmatrix} \tilde{\alpha}(x, t) \\ \tilde{\beta}(x, t) \end{pmatrix} &= \mathcal{T}(\tilde{z}(\cdot, t), \tilde{w}(\cdot, t)) - \begin{pmatrix} \Lambda(x) \\ \Lambda_1(x) \end{pmatrix} \tilde{v}_d(t) \\
&:= \mathcal{T}_1(\tilde{z}(\cdot, t), \tilde{w}(\cdot, t), \tilde{v}_d(t)) \quad (\text{E.12})
\end{aligned}$$

recalling (77), (78). According to (62), (79), we have the solution of the observer errors of the distal ODE, and the external signals are

$$\tilde{v}_r(t) = \tilde{v}_r(0)e^{(S_r - L_r \tilde{P}_r)t}, \quad (\text{E.13})$$

$$\begin{aligned} \tilde{v}_d(t) &= \tilde{v}_d(0)e^{(S_d - L_d \Lambda(1))t} \\ &- \int_0^t e^{(S_d - L_d \Lambda(1))(t-\tau)} L_d \tilde{\alpha}(1, \tau) d\tau, \end{aligned} \quad (\text{E.14})$$

for $t \in [t_0, \infty)$. It is known from (E.13) that

$$|\tilde{v}_r(t)| \leq M_0 M_r(t) e^{-\sigma_r t} \quad (\text{E.15})$$

for $t \in [t_0, \infty)$, where $M_r(t), \sigma_r$ are defined by Lemma 2 with applying $A_H = S_r - L_r \tilde{P}_r$, and where

$$M_0 = \sqrt{\sum_{i=n_d+1}^{n_v} (\bar{v}_i - \underline{v}_i)^2} \quad (\text{E.16})$$

recalling Assumption 4. According to (E.10) that shows that $\bar{\alpha} \equiv 0$ for $t \in [\frac{1}{q_1} + \frac{1}{q_2}, \infty)$, we also obtain from (79) that

$$\tilde{v}_d(t) = \tilde{v}_d\left(\frac{1}{q_1} + \frac{1}{q_2}\right) e^{(S_d - L_d \Lambda(1))(t - \frac{1}{q_1} - \frac{1}{q_2})}, \quad (\text{E.17})$$

for $t \in [\frac{1}{q_1} + \frac{1}{q_2}, \infty)$. Applying Lemma 2, we then obtain from (E.14), (E.17) that

$$\begin{aligned} |\tilde{v}_d(t)| &\leq M_1 \max_{\tau \in [0, \frac{1}{q_1} + \frac{1}{q_2}]} \|e^{(S_d - L_d \Lambda(1))\tau}\|_2 \\ &+ \left(\frac{1}{q_1} + \frac{1}{q_2}\right) |L_d| \max(\bar{\alpha}[t_0], \bar{\beta}[t_0]) \\ &\times \max_{\tau \in [0, \frac{1}{q_1} + \frac{1}{q_2}]} \|e^{(S_d - L_d \Lambda(1))\tau}\|_2 := M_d, \quad t \in [0, \frac{1}{q_1} + \frac{1}{q_2}), \end{aligned} \quad (\text{E.18})$$

$$|\tilde{v}_d(t)| \leq \check{M}_d M_2(t) e^{-\sigma_e t}, \quad t \in [\frac{1}{q_1} + \frac{1}{q_2}, \infty) \quad (\text{E.19})$$

where $\max(\bar{\alpha}[t_0], \bar{\beta}[t_0])$, whose exact value may be unaccessible because of the unknown initial states, can be replaced with its upper bound that can be obtained by applying (E.12) and the known bounds of the initial states in Assumptions 3, 4, and where $M_1 = \sqrt{\sum_{i=1}^{n_d} (\bar{v}_i - \underline{v}_i)^2}$ according to Assumption 4, and also

$$\check{M}_d = M_d \|e^{(S_d - L_d \Lambda(1))(\frac{1}{q_1} + \frac{1}{q_2})}\|_2, \quad (\text{E.20})$$

and $M_2(t), \sigma_e$ are defined by Lemma 2 with applying $A_H = S_d - L_d \Lambda(1)$. Note that $\tilde{v}_d(t)$ is exponentially convergent to zero considering the fact that $M_2(t)$ is a polynomial in t , the product of which and an exponentially decaying function (with an arbitrarily positive decay rate) will indeed converge to zero. Applying Cauchy-Schwarz inequality into the

transformations (77), (78), (68), (69), we have

$$\|\tilde{z}(\cdot, t)\| + \|\tilde{w}(\cdot, t)\| \leq \Upsilon_1 (\|\bar{\alpha}(\cdot, t)\| + \|\bar{\beta}(\cdot, t)\| + |\tilde{v}(t)|) \quad (\text{E.21})$$

for some positive Υ_1 that depends the kernel gains in the transformations (77), (78), (68), (69). According to (E.1)–(E.11), we have $\|\bar{\alpha}[t]\| + \|\bar{\beta}[t]\| \leq \|\bar{\alpha}[t_0]\| + \|\bar{\beta}[t_0]\|$ for $t \in [t_0, \frac{1}{q_1} + \frac{1}{q_2})$ and $\|\bar{\alpha}[t]\| + \|\bar{\beta}[t]\|$ is identically zero on $t \in [\frac{1}{q_1} + \frac{1}{q_2}, \infty)$. It is obtained from (E.21) that $\|\tilde{z}(\cdot, t)\| + \|\tilde{w}(\cdot, t)\| \leq \Upsilon_1 (\check{M}_d + |\tilde{v}(t)|)$, $t \in [t_0, \frac{1}{q_1} + \frac{1}{q_2})$ and $\|\tilde{z}(\cdot, t)\| + \|\tilde{w}(\cdot, t)\| \leq \Upsilon_1 |\tilde{v}(t)|$, $t \geq \frac{1}{q_1} + \frac{1}{q_2}$, where

$$\check{M}_d = \|\bar{\alpha}[t_0]\| + \|\bar{\beta}[t_0]\| \quad (\text{E.22})$$

whose upper bound can be obtained by (E.12) and the known bounds of the initial states in Assumptions 3, 4. Recalling (E.15), (E.18), (E.19), this lemma is obtained.

References

- [1] A. Aamo, "Disturbance rejection in 2×2 linear hyperbolic systems," *IEEE Trans. Autom. Control*, 58, 1095–1106, 2013.
- [2] Anfinsen, H., Aamo, O. "Disturbance rejection in general heterodirectional 1-D linear hyperbolic systems using collocated sensing and control," *Automatica*, 76, 230–242, 2017.
- [3] I. Abel, D. Steeves, M. Krstic, M. Jankovic, "Prescribed-time safety design for strict-feedback nonlinear systems," *IEEE Trans. Autom. Control*, 69(3): 1464–1479, 2023.
- [4] I. Abel, M. Jankovic, and M. Krstic, "Constrained control of multi-input systems with distinct input delays," *Int. J. Robust Nonlin.*, 34(10): 6659–6682, 2024.
- [5] A. D. Ames, X. Xu, J. W. Grizzle, and P. Tabuada, "Control barrier function based quadratic programs for safety critical systems," *IEEE Trans. Autom. Control*, 62(8):3861–3876, 2016.
- [6] M. Black, E. Arabi, and D. Panagou, "A fixed-time stable adaptation law for safety-critical control under parametric uncertainty," in *Proc. IEEE European Control Conf.*, pp. 1328–1333, 2021.
- [7] D. Bou. Saba, F. Bribiesca-Argomedo, M. D. Loreto and D. Eberard, "Strictly proper control design for the stabilization of 2×2 linear hyperbolic ODE-PDE-ODE systems," in *Proc. 58th IEEE Conf. Decis. Control*, pp. 4996–5001, 2019.
- [8] J.M. Coron, R. Vazquez, M. Krstic and G. Bastin, "Local exponential H^2 stabilization of a 2×2 quasilinear hyperbolic system using backstepping," *SIAM J. Control Optim.*, 51(3), pp. 2005–2035, 2013.
- [9] J. Deutscher, N. Gehring and R. Kern "Output feedback control of general linear heterodirectional hyperbolic ODE-PDE-ODE systems," *Automatica*, 95, pp. 472–480, 2018.
- [10] J. Deutscher, N. Gehring, R. Kern "Output feedback control of general linear heterodirectional hyperbolic PDE-ODE systems with spatially-varying coefficients," *Int. J. Control*, 92(10), pp.2274–2290, 2019.
- [11] J. Deutscher, "Output regulation for general linear heterodirectional hyperbolic systems with spatially-varying coefficients," *Automatica*, 85, pp.34–42, 2017.
- [12] J. Deutscher, J. Gabriel, "A backstepping approach to output regulation for coupled linear wave-ODE systems," *Automatica*, 123, 109338, 2021.

- [13] S. Koga, M. Krstic, “Safe PDE backstepping QP control with high relative degree CBFs: Stefan model with actuator dynamics,” *IEEE Trans. Autom. Control*, DOI: 10.1109/TAC.2023.3250514, 2023.
- [14] M. Krstic, A. Smyshlyaev, *Boundary control of PDEs*, SIAM, 2008.
- [15] M. Krstic, M. Bement, “Nonovershooting control of strict-feedback nonlinear systems,” *IEEE Trans. Autom. Control*, 51, pp. 1938–1943, 2006.
- [16] W. Li, M. Krstic, “Mean-nonovershooting control of stochastic nonlinear systems,” *IEEE Trans. Autom. Control*, 66 (12), pp: 5756–5771, 2020.
- [17] F. Di Meglio, F. Bribiesca-Argomedo, L. Hu and M. Krstic, “Stabilization of coupled linear heterodirectional hyperbolic PDE-ODE systems,” *Automatica*, 87, pp. 281–289, 2018.
- [18] Q. Nguyen and K. Sreenath, “Exponential control barrier functions for enforcing high relative-degree safety-critical constraints,” in *Proc. Amer. Control Conf.*, pp. 322–328, 2016.
- [19] R. Vazquez and M. Krstic, “Marcum Q -functions and explicit kernels for stabilization of 2×2 linear hyperbolic systems with constant coefficients,” *Syst. Control Lett.*, 68, pp. 33–42, 2014.
- [20] R. Vazquez, M. Krstic and J.M. Coron, “Backstepping boundary stabilization and state estimation of a 2×2 linear hyperbolic system,” in *50th IEEE Conference on Decision and Control and European Control Conference*, pp. 4937–4942, 2011.
- [21] J. Wang and M. Krstic, “Delay-compensated control of sandwiched ODE-PDE-ODE hyperbolic systems for oil drilling and disaster relief,” *Automatica*, 120, pp. 109131, 2020.
- [22] J. Wang and M. Krstic, *PDE Control of String-Actuated Motion*, Princeton University Press, 2022.
- [23] J. Wang, M. Krstic and Y. Pi, “Control of a 2×2 coupled linear hyperbolic system sandwiched between two ODEs,” *Int. J. Robust Nonlin.*, 28, pp. 3987–4016, 2018.
- [24] J. Wang and M. Krstic, “Output-positive adaptive control of hyperbolic PDE-ODE cascades,” arXiv:2309.05596v3, 2025.
- [25] W. Xiao and C. Belta, “Control barrier functions for systems with high relative degree,” in *Proc. Conf. Decis. Control*, pp. 474–479, 2019.
- [26] W. Xiao and C. Belta, “High order control barrier functions,” *IEEE Trans. Autom. Control*, 67(7), pp. 3655–3662, 2021.
- [27] X. Xu and S. Dubljevic, “Output regulation boundary control of first-order coupled linear MIMO hyperbolic PIDE systems,” *International Journal of Control*, 93(3), pp: 410–423, 2020.
- [28] J. Gabriel, J. Deutscher, “State feedback regulator design for coupled linear wave equations,” In *Proc. European Control Conference (ECC)*, Limassol, Cyprus, pp. 3013–3018, 2018.
- [29] J.-J. Gu, J.-M. Wang, Y.-P. Guo, “Output regulation of anti-stable coupled wave equations via the backstepping technique,” *IET Control Theory and Applications*, 12, 431–445, 2018.
- [30] A. Irscheid, J. Deutscher, N. Gehring, J. Rudolph, “Output regulation for general heterodirectional linear hyperbolic PDEs coupled with nonlinear ODEs,” *Automatica*, 148, 110748, 2023.
- [31] J. Redaud, F. Bribiesca-Argomedo, J. Auriol, “Output regulation and tracking for linear ODE-hyperbolic PDE-ODE systems,” *Automatica*, 162, 111503, 2024.
- [32] K. Yoshida, *Lectures on differential and integral equations*, volume 10. Interscience Publishers, 1960.